FILE COPY

N-1806

NCEL
Technical Note

January 1990

By T. Joseph Holland

Sponsored By Naval Facilities
Engineering Command

FINITE ELEMENT STUDY OF JOINT SEALS IN PORTLAND CEMENT CONCRETE PAVEMENTS

ABSTRACT Pavement seal behaviors were investigated using the finite element method to obtain a better understanding of their failure mechanisms. This knowledge is needed to explain failures that actually occur in the field and may help to reduce joint seal costs, which are estimated to be $12M annually. The effects of width, depth, and size were evaluated and compared with parabolic predictions. The finite element results indicated that the assumption of a parabolic free surface upon expansion was not applicable in all cases and the strains were not uniform. The finite element results consistently showed high strains at the vertical pavement-joint seal interface, suggesting that failures should occur there first in properly designed joints.

NAVAL CIVIL ENGINEERING LABORATORY PORT HUENEME CALIFORNIA 93043-5003

METRIC CONVERSION FACTORS

Approximate Conversions to Metric Measures

Symbol	When You Know	Multiply by	To Find	Symbol
		LENGTH		
in	inches	*2.5	centimeters	cm
ft	feet	30	centimeters	cm
yd	yards	0.9	meters	m
mi	miles	1.6	kilometers	km
		AREA		
in^2	square inches	6.5	square centimeters	cm^2
ft^2	square feet	0.09	square meters	m^2
yd^2	square yards	0.8	square meters	m^2
mi^2	square miles	2.6	square kilometers	km^2
	acres	0.4	hectares	ha
		MASS (weight)		
oz	ounces	28	grams	g
lb	pounds	0.45	kilograms	kg
	short tons (2,000 lb)	0.9	tonnes	t
		VOLUME		
tsp	teaspoons	5	milliliters	ml
Tbsp	tablespoons	15	milliliters	ml
fl oz	fluid ounces	30	milliliters	ml
c	cups	0.24	liters	l
pt	pints	0.47	liters	l
qt	quarts	0.95	liters	l
gal	gallons	3.8	liters	l
ft^3	cubic feet	0.03	cubic meters	m^3
yd^3	cubic yards	0.76	cubic meters	m^3
		TEMPERATURE (exact)		
°F	Fahrenheit temperature	5/9 (after subtracting 32)	Celsius temperature	°C

*1 in = 2.54 (exactly). For other exact conversions and more detailed tables, see NBS Misc. Publ. 286, Units of Weights and Measures, Price $2.25, SD Catalog No. C13.10:286.

Approximate Conversions from Metric Measures

Symbol	When You Know	Multiply by	To Find	Symbol
		LENGTH		
mm	millimeters	0.04	inches	in
cm	centimeters	0.4	inches	in
m	meters	3.3	feet	ft
m	meters	1.1	yards	yd
km	kilometers	0.6	miles	mi
		AREA		
cm^2	square centimeters	0.16	square inches	in^2
m^2	square meters	1.2	square yards	yd^2
km^2	square kilometers	0.4	square miles	mi^2
ha	hectares (10,000 m^2)	2.5	acres	
		MASS (weight)		
g	grams	0.035	ounces	oz
kg	kilograms	2.2	pounds	lb
t	tonnes (1,000 kg)	1.1	short tons	
		VOLUME		
ml	milliliters	0.03	fluid ounces	fl oz
l	liters	2.1	pints	pt
l	liters	1.06	quarts	qt
l	liters	0.26	gallons	gal
m^3	cubic meters	35	cubic feet	ft^3
m^3	cubic meters	1.3	cubic yards	yd^3
		TEMPERATURE (exact)		
°C	Celsius temperature	9/5 (then add 32)	Fahrenheit temperature	°F

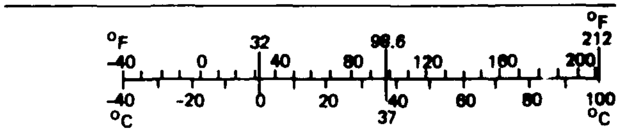

REPORT DOCUMENTATION PAGE

Form Approved
OMB No. 0704-0188

1. AGENCY USE ONLY (*Leave blank*)	2. REPORT DATE	3. REPORT TYPE AND DATES COVERED
	January 1990	Final — Sep 88 to Aug 89

4. TITLE AND SUBTITLE

FINITE ELEMENT STUDY OF JOINT SEALS IN PORTLAND CEMENT CONCRETE PAVEMENTS

5. FUNDING NUMBERS

PE — 63725N
WU — DN668078

6. AUTHOR(S)

T. Joseph Holland

7. PERFORMING ORGANIZATION NAME(S) AND ADDRESS(ES)

Naval Civil Engineering Laboratory
Port Hueneme, CA 93043-500?

8. PERFORMING ORGANIZATION REPORT NUMBER

TN-1806

9. SPONSORING/MONITORING AGENCY NAME(S) AND ADDRESS(ES)

Naval Facilities Engineering Command
Alexandria, VA 22332

10. SPONSORING/MONITORING AGENCY REPORT NUMBER

11. SUPPLEMENTARY NOTES

12a. DISTRIBUTION/AVAILABILITY STATEMENT

Approved for public release; distribution is unlimited.

12b. DISTRIBUTION CODE

13. ABSTRACT (*Maximum 200 words*)

Pavement seal behaviors were investigated using the finite element method to obtain a better understanding of their failure mechanisms. This knowledge is needed to explain failures that actually occur in the field and may help to reduce joint seal costs, which are estimated to be $12M annually. The effects of width, depth, and size were evaluated and compared with parabolic predictions. The finite element results indicated that the assumption of a parabolic free surface upon expansion was not applicable in all cases and the strains were not uniform. The finite element results consistently showed high strains at the vertical pavement-joint seal interface, suggesting that failures should occur there first in properly designed joints.

14. SUBJECT TERMS

Pavement seals, polysulfide seals, silicone seals, rubberized asphalt seals, finite element method, hyperelastic models , (KR)

15. NUMBER OF PAGES

40

16. PRICE CODE

17. SECURITY CLASSIFICATION OF REPORT	18. SECURITY CLASSIFICATION OF THIS PAGE	19. SECURITY CLASSIFICATION OF ABSTRACT	20. LIMITATION OF ABSTRACT
Unclassified	Unclassified	Unclassified	UL

CONTENTS

INTRODUCTION

The purpose of this study was to evaluate the influences of the joint width and depth on seal behavior and failure mechanisms using finite elements and comparing them with the simplified techniques of Reference 1. Understanding of the failure mechanisms and modes is needed to explain failures that actually occur in the field and may help to reduce joint seal costs, which are estimated to be $12M annually. The ABAQUS finite element program (Ref 2) was used to calculate the joint seal responses to various pavement expansions.

Egons Tons (Ref 1) proposed an analytical means for evaluating pavement seal behavior. The basic assumptions made in Reference 1 include:

1. The joint cross section is rectangular.

2. The sealer is a liquid-type homogeneous compound which cannot change in volume but changes shape in response to joint extensions.

3. The free surface curves after extension are parabolic.

4. The free surface curves after extension are the same for both the top and bottom.

5. The minimum and maximum joint extensions are the indicators of the total strains in the sealer.

6. The strain in the sealer along the free surface parabolic curve is uniformly distributed.

Reference 1 also implies that the maximum strain occurs along the free surface parabolic curve. The terms associated with the parabolic curve are given in Figure 1. Using the above assumptions Reference 1 evaluates the influences of the joint width and depth and then compares them to experimental results.

In the finite element analysis assumptions 1, 2, 4, and 5 of Reference 1 were used. Assumption 3, stating that the free surface assumes a parabolic shape upon extension, is not enforced with the finite element analysis. Eight-node quadrilateral elements with quadratic interpolation were used. These elements are capable of modelling a parabola on the free surface if that is what equilibrium dictates, but they are not restricted to it. In the finite element analysis the strain distribution is computed element by element and therefore the assumption (no. 6) that the strain is uniformly distributed along the free surface is not enforced. Also, all strains are evaluated in the finite element analysis so that the maximum strains may not necessarily occur on the free surface.

ELASTIC CALCULATIONS

Evaluations were made of the finite element mesh of the pavement seal using linear elastic elements. A symmetric quarter (or a 1/8- by 1/8-inch section) of a 1/4- by 1/4-inch rectangular seal was modeled with a 10 by 10 element mesh (see Figure 2). Eight-node elements were chosen because the curvature of the free surface of the deformed model was expected to be nearly parabolic. The plane strain formulation was used because the seal is modeled as a perpendicular slice of a long section of the pavement seal. The pavement edge is defined as rigid with perfect bond to the seal (i.e., the seal can rotate but not translate). The centerline surfaces were modeled with symmetric boundaries. The finite element model was subjected to an extension of 50 percent (1/8 inch). Using Reference 1, the expected depth of the parabola is H = -0.0625 inches and the maximum strain is $S_{max} = 0.60$.

Four calculations were made using a Young's modulus of 10 psi, various Poisson's ratios (υ), and an elastic formulation which is applicable only for small strains (i.e., $\varepsilon << 1$). These calculations were made to evaluate the mesh and how compressibility (i.e., Poisson's ratio) influences the behavior. The Poisson's ratio included: 0.0,. 0.3, 0.49, and 0.50.

Figure 3 shows the free surface deformation as calculated by Reference 1 (parabola) and the finite element method (FE results). As the Poisson ratio increases the indentation increases. Although the magnitudes are different, the predicted shapes are closely approximated by the parabolic shape described by Reference 1. The strains calculated by the finite element method on the free surface are shown in Figure 4. Near the center of the seal, all of the finite element results tend to converge and remain nearly uniform. Near the pavement edge, however, the finite element results indicate a sharp increase in strains.

An additional calculation was made with this elastic formulation but included geometric nonlinearities (where stress and strain depend upon the deformed position). The plot of the free surface is shown in Figure 5 and shows a significant departure from the parabolic shape. The free surface predicted using geometric nonlinearities "curves in" more near the edge and tends to "flatten out" near the middle resulting in a smaller indentation.

PAVEMENT SEALS

Hyperelastic Model Parameters

The hyperelastic material model in ABAQUS (Ref 2) was used for modeling the pavement seals. This model incorporates both large strain formulation and geometric nonlinearities. For this study, an incompressible material was assumed although compressibility can be incorporated. A literature review revealed very little test data (e.g., stress-strain) on pavement seals. Reference 3 provided some tensile tests of several types of seals (see Figure 6). To get a representative sample of seal behavior, three types of seals were chosen for analysis: (1) rubberized asphalt, (2) silicone, and (3) polysulfide. ABAQUS (Ref 2) has curve

fitting procedures within the program for fitting the hyperelastic model parameters to the tensile test results. The results of this parameter fitting are given in Table 1.

Hyperelastic Model Tests

Finite element calculations using the hyperelastic material model were made using the same mesh as the elastic calculations (see Figure 2). The three pavement seal types were modeled with the incompressible hyperelastic model and given a horizontal extension of 1/8 inch (50 percent). Reference 1 gives, for any 1/4- by 1/4-inch pavement seal subjected to a 50 percent extension, an indentation (H = 0.0625 inches) and a strain along the surface (S_{max} = 0.60). The free surface deformation calculated by the finite element models was nearly the same for all of the seal types and is compared with the predicted parabola in Figure 7. The finite element results indicate a greater curvature of the free surface near the pavement edge and an indentation at the center is less than the parabola. This is similar to the elastic calculation with geometric nonlinearities (Figure 5). The extension strains along the free surface were calculated by the various finite element models and were nearly the same. These are compared to the 0.60 uniform distribution predicted by Reference 1 and are shown in Figure 8. The results indicate large strains at the pavement edge that rapidly decay a short distance from the pavement then steadily increase toward the centerline. The strains are all above the predicted value of 0.60.

Contour plots from the finite element calculations indicated that the strains everywhere were the same for all models. Contours of the extension strain, E11; the vertical strain, E22; and the shear strain, E12 are shown in Figures 9, 10, and 11, respectively. The largest strain (e.g., 3.1) is in the extension direction and occurs at the corner of the free surface and the pavement. All of these plots indicate large gradients near this corner.

The similarities in strains between the different materials can be explained in terms of the constraints on the mesh. The pavement edge is completely constrained, both the vertical and horizontal centerlines only allow sliding, and the incompressibility constraint and plane strain formulation allow no extension in the long direction (out of the plane of the paper). Kinematically, the material can only respond in a limited fashion. The stresses, however, do vary with the material type. The maximum principal stresses range from 110 psi in the polysulfide, 60 psi in the silicone, and 50 psi in the rubberized asphalt. The maximum stresses all occur at the corner of the pavement and the free surface.

Finite Element Meshes

Both the elastic and hyperelastic finite element analyses indicated that there was a large gradient in terms of strain and stress at the corner of the free surface and pavement. The uniform mesh (Figure 2) and two other meshes were examined to determine whether a finer mesh is required to capture the gradient. The polysulfide hyperelastic material was used as a basis for evaluating the meshes. Mesh 2 uses the same number of elements but condenses them near the corner (Figure 12). Mesh 3 subdivides every element in mesh 2 by four (Figure 13).

Each mesh was subjected to a horizontal extension of 1/8 inch (50 percent). The free surface deformation showed a marked difference from a parabolic assumption but little difference between the meshes (Figure 14). The vertical strains (E22), and the shear strains (E12) show virtually no differences between the meshes. The extension strain (E11) shows no differences between the meshes except at the corner node at the intersection of the free surface and the pavement. Figure 15 shows the E11 strain on the free surface for each of the meshes (compared to the 0.60 calculated by Reference 1). As the element near the corner is reduced with each succeeding mesh, the strains at the corner increase dramatically. Strains everywhere else on the surface show little difference between the meshes (Figure 15). The principal strains at the corner are given in Table 2. The maximum principal strain increases as the corner element is reduced in each succeeding mesh. The minimum principal strain and the angle, however, show little difference between the meshes. The extension strain (E11) for each of the meshes is compared at levels slightly below the surface. The strain at 0.00625 inches below the surface is shown in Figure 16 and at 0.0125 inches below surface in Figure 17. The strains at these levels are essentially the same for all meshes. Figures 15, 16, and 17 all show the same basic shape: high strains near the pavement that drop rapidly, then steadily increase toward the centerline. This shape similarly appears in the other materials (Figure 8).

Contour plots of the E11 strain were made for all of the meshes (a typical plot is shown in Figure 18). These plots indicated that the E11 strain was the same everywhere for all of the meshes, except right at the corner node.

The high strain in the corner region appears to be a realistic response of the seal as it is subjected to extension. Figures 15, 16, and 17 show a consistent increase in strain near the corner. The peak value at the corner node, however, varies with the mesh (Table 2). This variation in the strain at the corner node can be partially explained in that as the meshes are refined the element size is reduced and therefore the integration points are closer to the corner.

Influence of Seal Width

Two different widths were examined to determine the initial width influence on the strains. The symmetric quarter of a 1/4- by 1/4-inch seal modeled with mesh 2 (Figure 12) was used as the baseline and compared to a seal 1/4 inch deep with a 1/2-inch initial width (Figure 19). Two calculations were made: (1) the 1/4- by 1/2-inch seal was subjected to a 1/8-inch extension (25 percent), and (2) the 1/4- by 1/2-inch seal was subjected to a 1/4-inch extension (50 percent).

The results for the 1/4- by 1/2-inch seal subjected to a 1/8-inch extension are given in Table 3. The results for the 1/4- by 1/2-inch seal subjected to 1/4-inch extension (50 percent) are given in Table 4. In both tables the extension strain (E11) is given at the corner and on the surface at the centerline. Although the corner node strain is questionable, it is used here as a comparison between different widths and depths. The corner element is the same size for all of the meshes

used in the comparisons. Both tables indicate the reductions are consistent for the finite element strains and the uniform strain predicted by Reference 1 as the width is increased.

The free surface shapes for both the parabolic prediction and the finite element results for 1/8-inch and 1/4-inch extensions are shown in Figure 20. This plot shows a greater deviation of the finite element results from the parabolic shape as the extension is increased. The strains computed by finite elements on the free surface for both extensions are shown in Figure 21. It can be seen in Figure 21 that the surface strains have the same basic shape as the 1/4- by 1/4-inch seal surface strains (Figure 15).

Influence of Seal Depth

Two different depths were examined to determine the influence of depth on the strains. The 1/4- by 1/4-inch seal was again used as the baseline and compared to a seal 1/2 inch deep and with a 1/4-inch initial width (Figure 22). The corner element where high strains occur is the same size for both meshes. A calculation was made for an extension of 1/8 inch (50 percent).

The results for the 1/2- by 1/4-inch seal compared to the 1/4- by 1/4-inch seal are given in Table 5. These results show a predicted increase in strains via Reference 1 of 45 percent. The predicted increase via the finite element method varied, depending on location, from 4 to 70 percent. The free surface deformations computed by finite elements and the parabolic prediction are shown in Figure 23. It appears from this plot that as the depth increases (in relation to the width), the free surface more closely resembles the parabolic prediction. The strains computed by finite elements on the free surface are shown in Figure 24. The strains appear uniform near the centerline and then increase toward the pavement edge. This shape is slightly different than the previous surface strains (Figures 8, 15, and 21) in that it is more uniform near the centerline.

Influence of Seal Size

A larger seal was examined to determine the effects of the seal size on the strain distribution. The baseline mesh for the 1/4- by 1/4-inch seal (Figure 12) was increased to model a 1/2- by 1/2-inch seal (see Figure 25). The corner element where the high strains occur is the same size for both meshes. The calculation on the 1/2- by 1/2-inch seal was made for an extension of 1/4 inch (50 percent).

The results for the 1/2- by 1/2-inch seal compared to the 1/4- by 1/4-inch seal are given in Table 6. Reference 1 predicts no change in maximum strain between the seals. The finite element results indicate that there is little change in the centerline strain but shows an increase of 31 percent in the strain at the corner. The free surface deformations computed by finite elements and the parabolic prediction are shown in Figure 26. The strains computed by finite elements are shown in Figure 27. Both figures show the same basic shapes computed

for the 1/4- by 1/4-inch seal (see Figures 14 and 15). The extension strain (E11) contours are shown in Figure 28 and show virtually no difference from the 1/4- by 1/4-inch results (Figure 18).

CONCLUSIONS

The finite element calculations provide some useful insights on the behavior of pavement seals. Indications are that some of the early assumptions on seal behavior (Ref 1) may not be adequate for a large range of extensions. Specifically, the two assumptions that the free surface shape is parabolic (no. 3) and the strain is uniform along the surface (no. 6) aren't accurate for all extensions.

Results from the 1/4- by 1/4-inch and the 1/4- by 1/2-inch seal extensions (Figures 5, 7, 14, and 20) indicate that the seal has a greater curvature near the pavement edge than the parabolic shape assumes. The constant volume assumption (no. 2) is still maintained in the finite element calculations because of the material models used; thus, the indentation at the centerline is less. The elastic calculations demonstrated that the effects of geometric nonlinearities played a major role in the free surface deviating from the parabolic shape (Figures 3 and 5). The parabolic shape, however, seems to provide an adequate approximation for deeper seals (Figure 23).

The assumption of a uniform strain along the surface (no. 6) doesn't appear to be valid for any of the extensions (Figures 8, 15, 21, 24, and 27). Even slightly below the surface, basic nonuniform strain shapes emerge (Figures 16 and 17). The peak strain at the corner of the free surface and pavement appears to be mesh sensitive. High strains in the seal near this corner do exist; however, the exact value is in question. This is confirmed by both the strains taken at slightly below the surface (Figures 16 and 17) and all of the strain contours (Figures 9, 10, 11, 18, and 28). It is expected that this peak value will also be sensitive to the compressibility of the seal material (the seal is modeled in this study as incompressible) and the boundary conditions (the pavement edge-seal bond is perfect).

Two basic shapes emerge from the surface strains: (1) the peak at the corner with a steady increase toward the center as shown in Figures 8, 15, 21, and 27, and (2) the peak of the corner and becoming uniform toward the center as shown in Figure 24. Except for the corner, the other high strain area (though not as high) occurs at the center of the seal (on the inside) as shown by the contour plots in Figures 9 and 18. Excluding the peak strain at the corner, the results appear to be independent of mesh sizes chosen in this study.

The interpretation of the results of this study, though limited, for practical application is that failures in joint seals should occur first at the pavement edge-seal interface. This is justified by the existence of high strains near the corner of the pavement edge and free surface (Figures 9, 18, and 28). Also, the pavement-seal bond would be less than the material bond. If failure occurs elsewhere (e.g., near the centerline) then, based upon the finite element results, this is an indication of an inferior material or improper design.

Reference 1 (published in 1959) provided a useful tool in analyzing and designing pavement seals. Now with modern computers and finite element technology, a more accurate picture of their behavior and failure mechanisms can be resolved by relaxing some of the assumptions made in Reference 1. Stresses and strains can be evaluated not only on the surface but anywhere in the interior. Further studies coupled with experimental testing can reduce some of the assumptions (see Recommendations) made in this study for the finite element calculations. With insights created by better assumptions and a larger data base of finite element calculations and experimental tests, a more accurate design procedure can be established.

RECOMMENDATIONS

1. A more accurate approximation of the peak strain value that occurs at the corner of the free surface and the pavement needs to be established. Its sensitivity to mesh size, boundary conditions, variation in seal shape, and material compressibility should be evaluated and compared with test results.

2. Material compressibility may significantly influence the strains throughout the seal as it is extended. Test evaluations may be needed since there is no evidence in the literature that volumetric tests have ever been conducted. Depending on whether it is beneficial, the compressibility may be something that can be externally controlled (e.g., air entrainment).

3. The adhesion (boundary conditions) of the seal material to the pavement should be investigated more thoroughly. The various materials used as pavement seals will bond differently to different pavements. Also, the failure mechanism of the pavement-material interface could be significantly different from a pure material failure. Partial yielding along the pavement-material interface could significantly influence strains throughout the seal and change the failure mechanisms. This is something that can easily be modeled by the finite element method.

4. Various initial seal shapes should be evaluated to determine their influence in the strains. A rectangular shape was assumed for this study but other shapes may result due to field applications (see Figure 29).

5. Time dependence of the seal material has not been mentioned in this study but is a real world effect. The high shear strains (Figure 11) in a viscous material might exist for rapid expansions, but pavements tend to expand and contract over a period of time. This period of time might be enough to allow for a relaxation of these shear strains and hence principle strains. A thorough literature search and/or a test program would provide the data necessary to model the time dependence. The finite element method could easily incorporate this time dependence for analysis.

6. Finally, a larger database of finite element calculations coupled with experimental tests could provide the basis for a simplified design procedure. This procedure might exist on a personal computer where a database of common pavement seal materials might also be kept.

REFERENCES

1. Egons Tons. "A theoretical approach to design of a road joint seal." Highway Research Board Bulletin No. 229, Jan 1959, pp 20-53.

2. Hibbitt, Karlsson, and Sorensen, Inc. ABAQUS User's Manual, Version 4.6, Providence, RI, 1987.

3. University of Texas. Research Report 385-1 (Project 3-18-84-385): Improved methods for sealing joints in Portland cement concrete pavements, by Alexander M. Collins III, Wayne D. Mangum, David W. Fowler and Alvin H. Meyer. Center for Transportation Research, Bureau of Engineering Research, Austin, TX, Sep 1986.

Table 1. Hyperelastic Model Parameters Derived with ABAQUS Curve Fitting Procedure on Data of Figure 6.

Material	Hyperelastic Model Parameters	
	C_{10}	C_{01}
Rubberized Asphalt	-0.4478	3.352
Silicone	0.2734	3.942
Polysulfide	2.895	4.472

Table 2. Principal Strains at the Corner Node for 50% Extension

Description	Element Edge Length (in.)	Maximum Principal Strain (in./in.)	Minimum Principal Strain (in./in.)	Angle (deg)
Mesh 1	0.0125	3.5180	-0.4225	-18.6
Mesh 2	0.00625	4.6317	-0.4448	-16.7
Mesh 3	0.003125	5.9390	-0.8200	-14.3

Table 3. Influence of Width for 1/8-Inch Extension

Parameter	1/4- by 1/4-Inch Seal	1/4- by 1/2-Inch Seal	Reduction (%)
Depth (in.)	1/4	1/4	
Width (in.)	1/4	1/2	
Extension (in.)	1/8	1/8	
Extension (%)	50	25	
Maximum strain (in./in.)(Ref 1)	0.60	0.26	-57
Extension strain (corner) (Finite element)	4.213	1.679	-60
Extension strain (centerline) (Finite element)	0.803	0.328	-59

Table 4. Influence of Width for 1/4-Inch Extension

Parameter	1/4- by 1/4-Inch Seal	1/4- by 1/2-Inch Seal	Reduction (%)
Depth (in.)	1/4	1/4	
Width (in.)	1/4	1/2	
Extension (in.)	1/8	1/4	
Extension (%)	50	50	
Maximum strain (in./in.)(Ref 1)	0.60	0.53	-12
Extension strain (corner) (Finite element)	4.213	3.582	-15
Extension strain (centerline) (Finite element)	0.803	0.747	-7

Table 5. Influence of Depth for 1/8-Inch Extension

Parameter	1/4- by 1/4-Inch Seal	1/4- by 1/2-Inch Seal	Increase (%)
Depth (in.)	1/4	1/2	
Width (in.)	1/4	1/4	
Extension (in.)	1/8	1/8	
Extension (%)	50	50	
Maximum strain (in./in.)(Ref 1)	0.60	0.87	45
Extension strain (corner) (Finite element)	4.213	7.178	70
Extension strain (centerline) (Finite element)	0.803	0.833	4

Table 6. Influence of Seal Size for 50% Extension

Parameter	1/4- by 1/4-Inch Seal	1/2- by 1/2-Inch Seal	Increase (%)
Depth (in.)	1/4	1/2	
Width (in.)	1/4	1/2	
Extension (in.)	1/8	1/4	
Extension (%)	50	50	
Maximum strain (in./in.)(Ref 1)	0.60	0.60	0
Extension strain (corner) (Finite element)	4.213	5.522	31
Extension strain (centerline) (Finite element)	0.803	0.801	-0.2

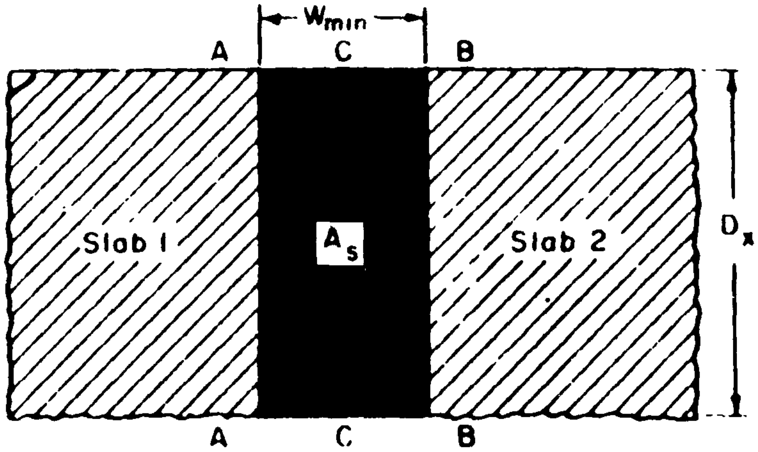

Sealed Joint at Minimum Width

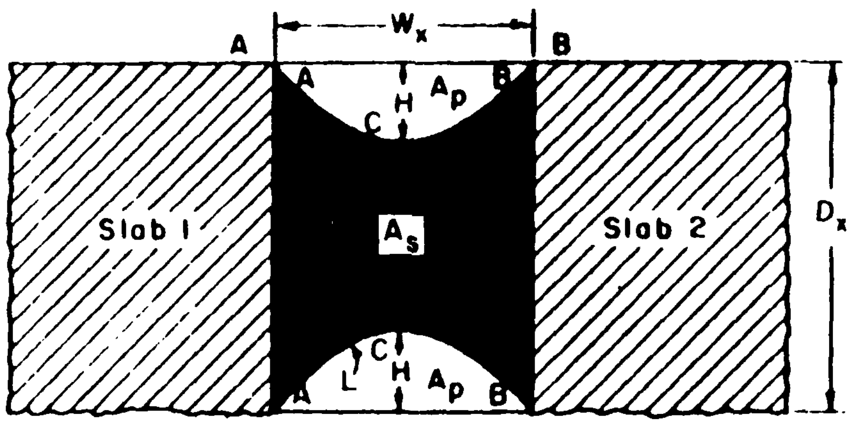

Sealed Joint after Expansion

W_{min} = minimum joint width

W_x = joint width of any extension

D_x = depth of sealer in the joint

H = maximum depth of the parabolic curve-in line

L = length of the parabolic arc (line ACB)

A_s = cross-sectional area of the sealer

A_p = area of the parabola ABC

ΔW = amount of joint expansion, in percent

S_{max} = amount of maximum strain in the sealer

Figure 1. Free surface prediction using parabolic method for a pavement seal subjected to extension.

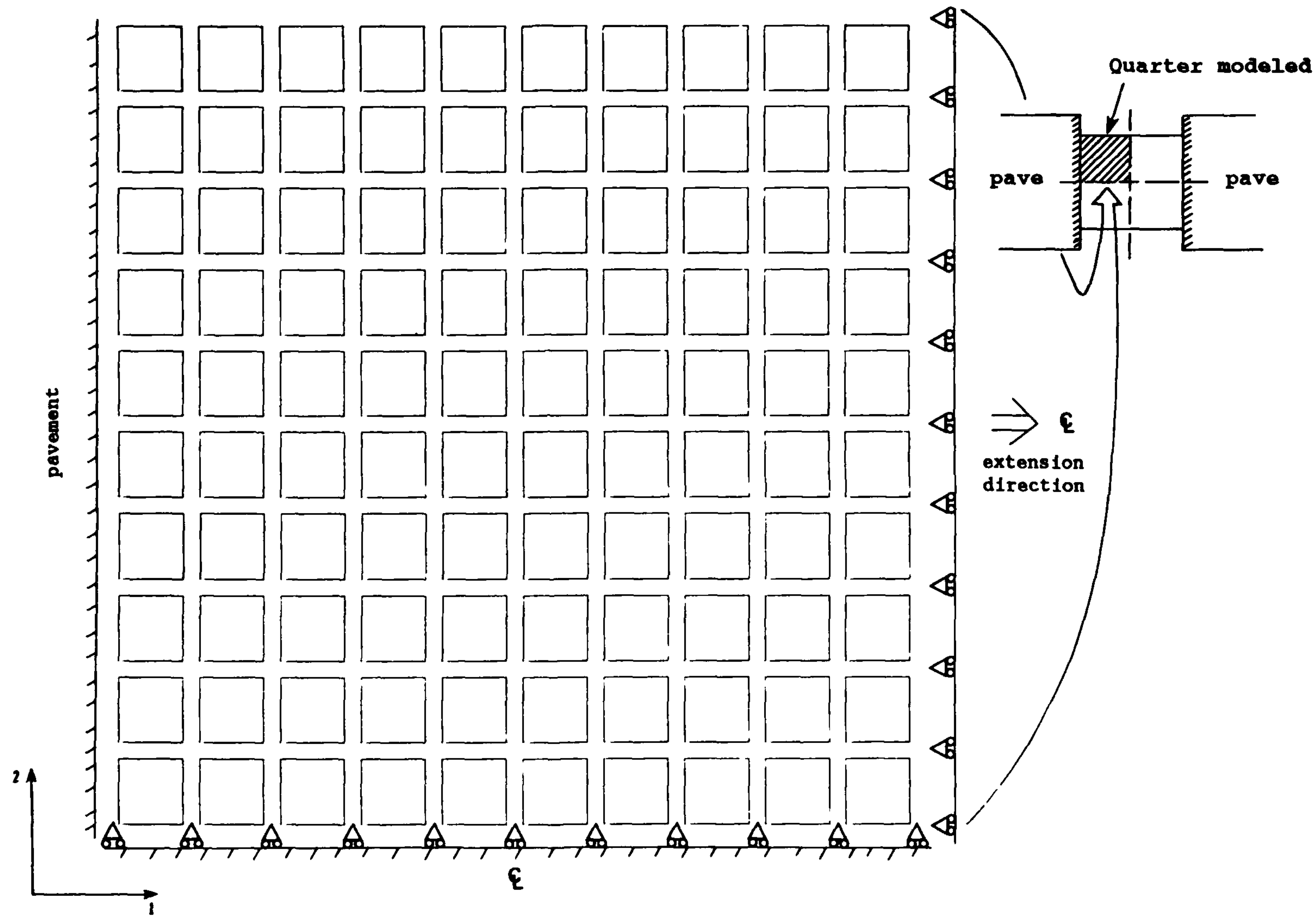

Figure 2. 10 by 10 finite element mesh of a 1/4- by 1/4-inch pavement seal (symmetric quarter).

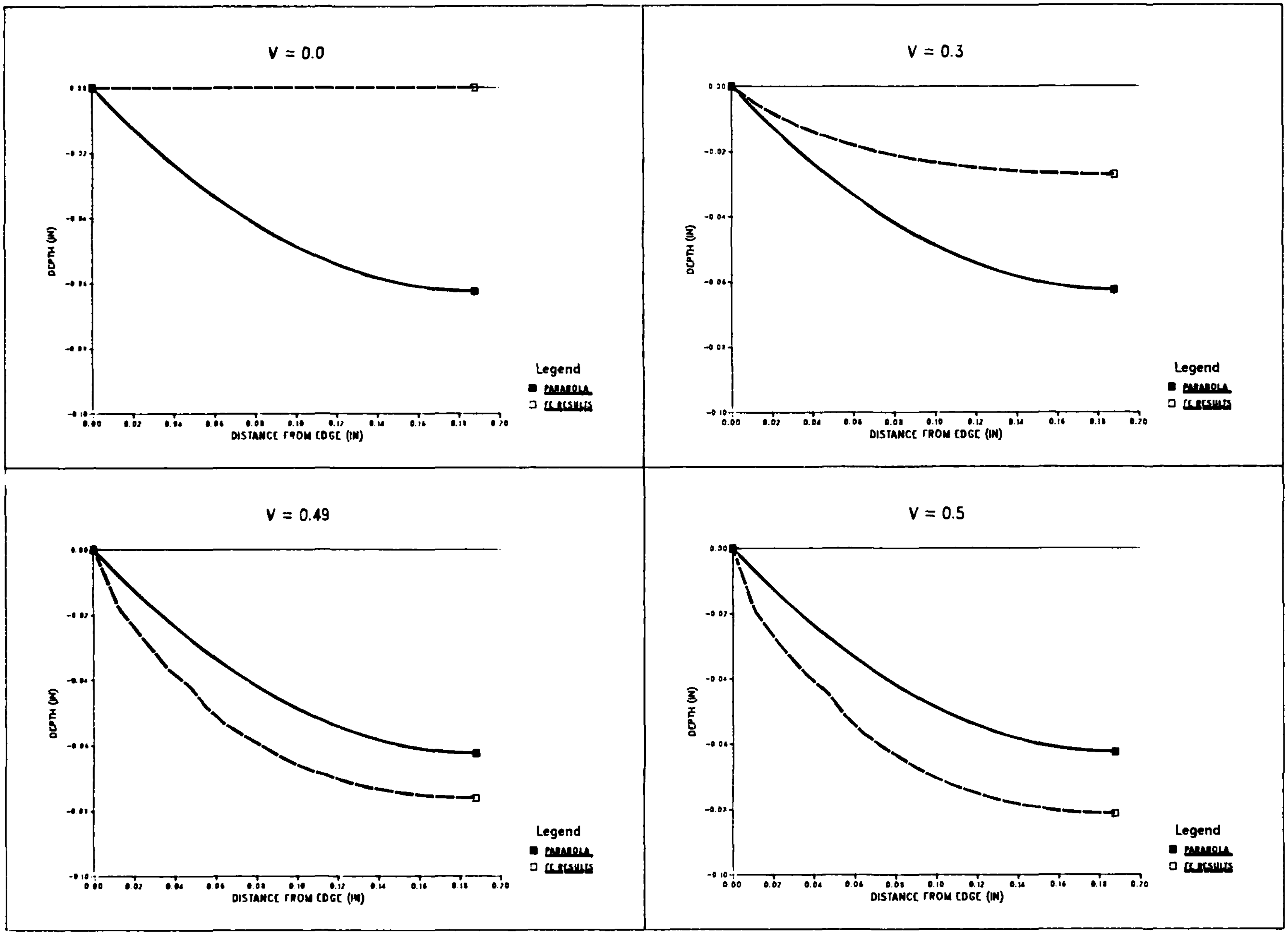

Figure 3. Free surface deformations from small strain, elastic calculations and various Poisson's ratios.

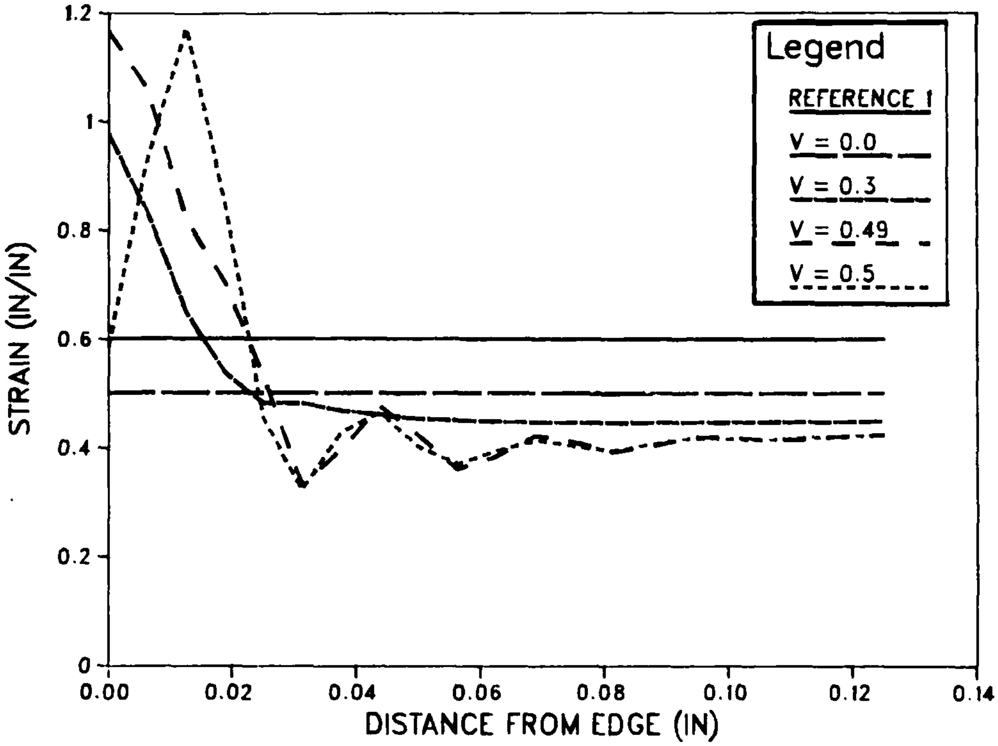

Figure 4. Strains on free surface from small strain, elastic calculations and various Poisson's ratios.

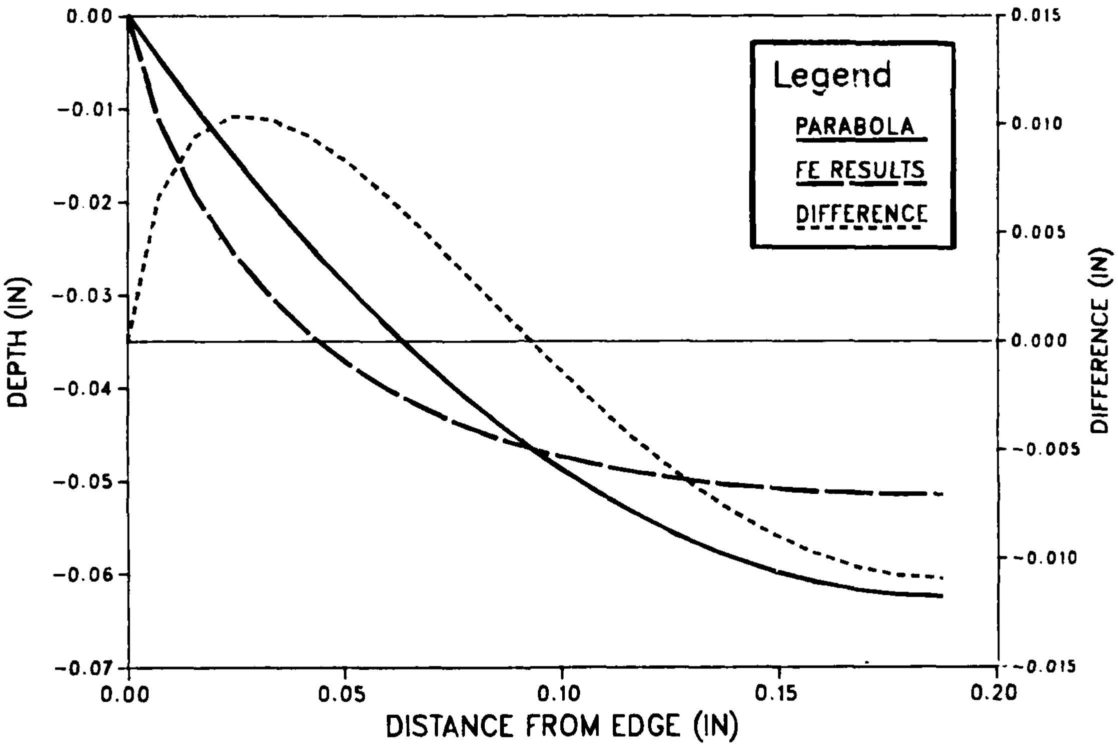

Figure 5. Free surface deformation from elastic calculations and geometric nonlinearity.

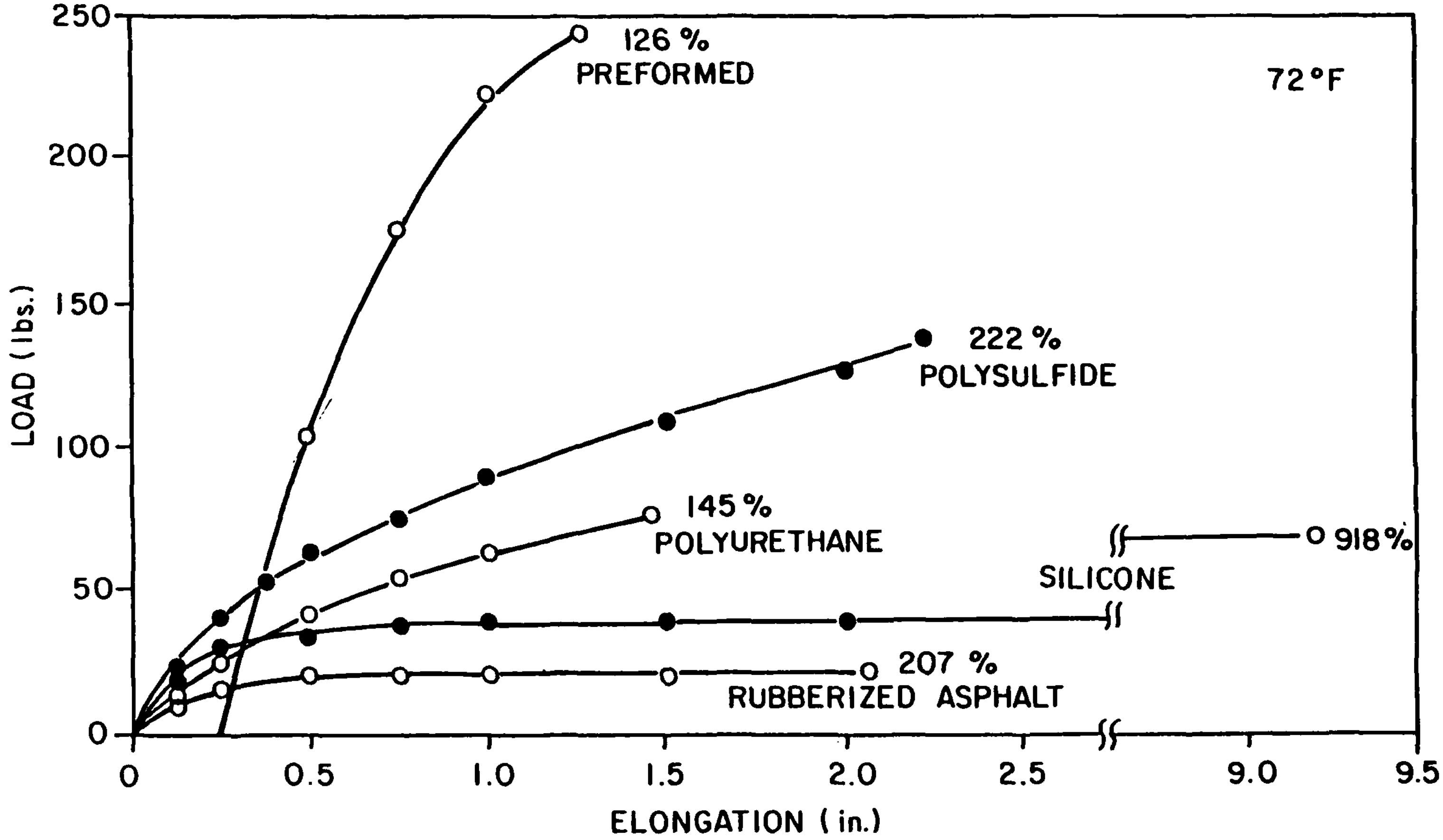

Figure 6. Load versus elongation curves for various materials (Ref 3).

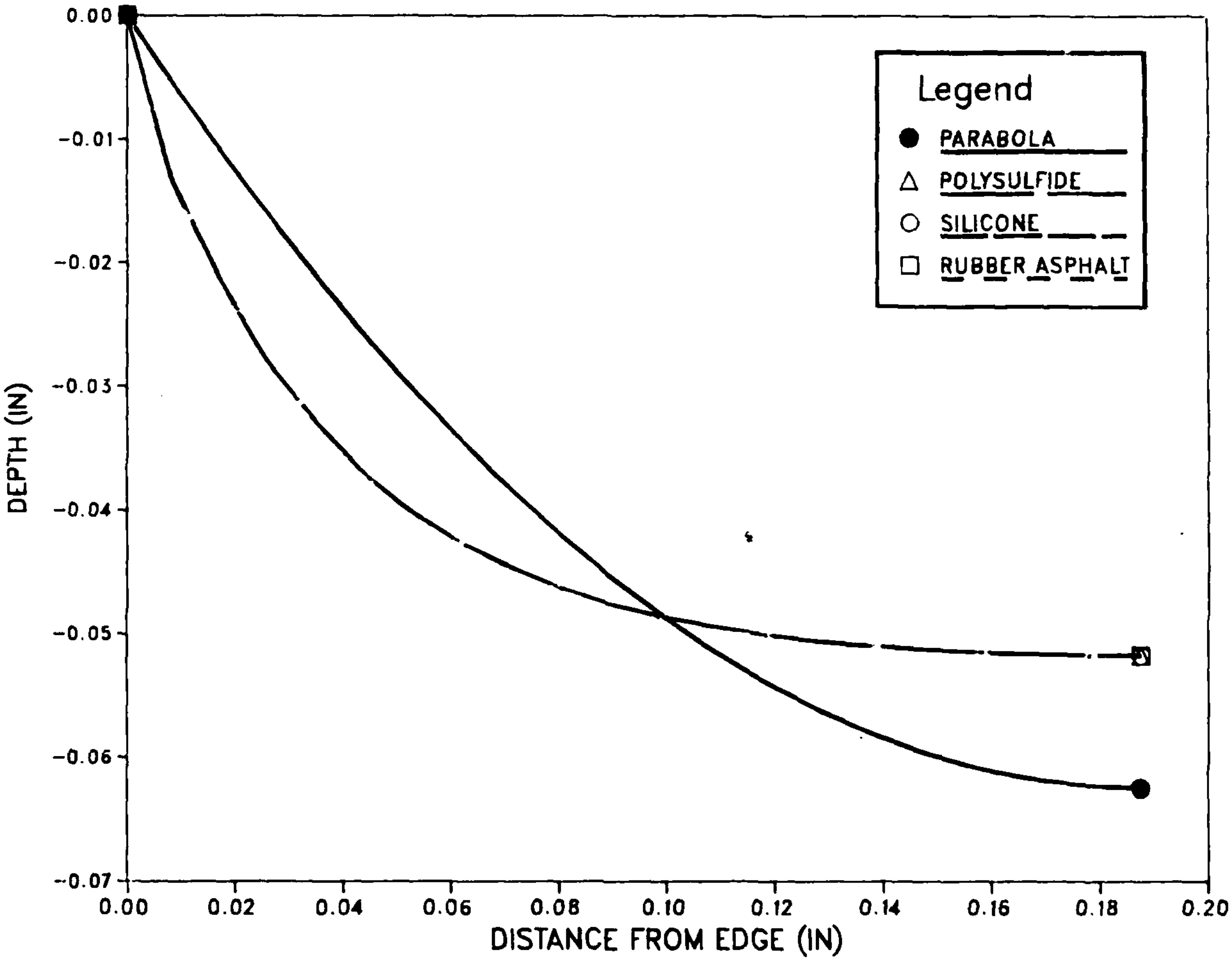

Figure 7. Free surface deformation for various seal materials at an extension of 50%.

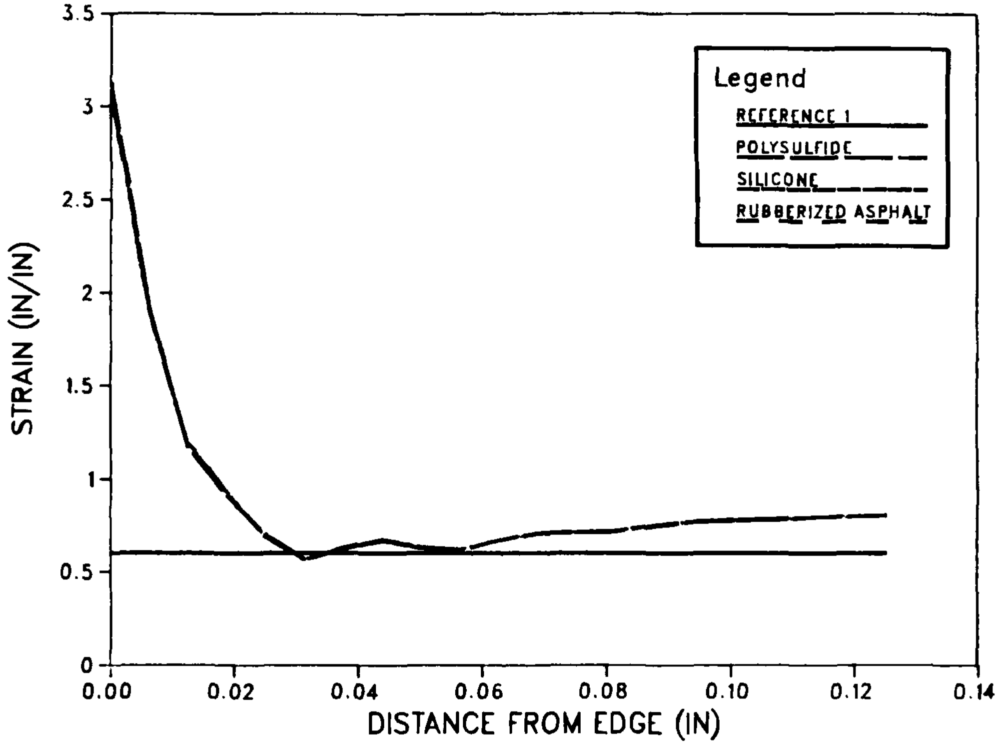

Figure 8. Strains on free surface for various seal materials at an extension of 50%.

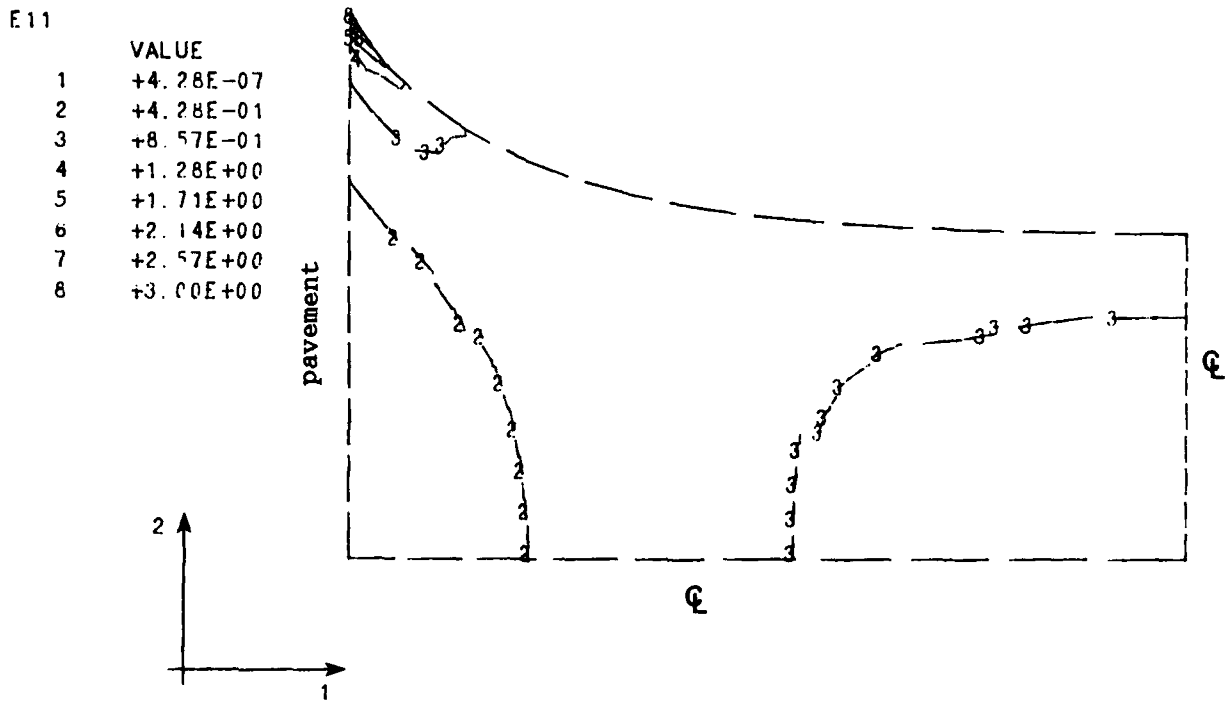

Figure 9. Strain in extension direction (E11) for an extension of 50%.

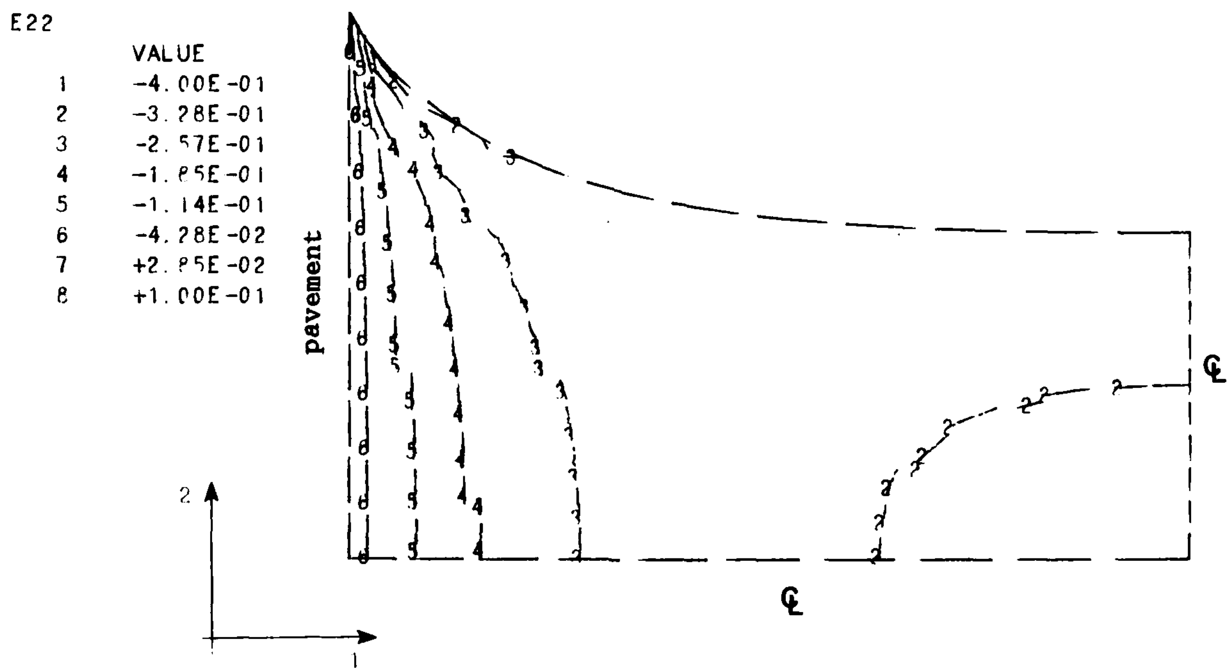

Figure 10. Strain in vertical direction (E22) for an extension of 50%.

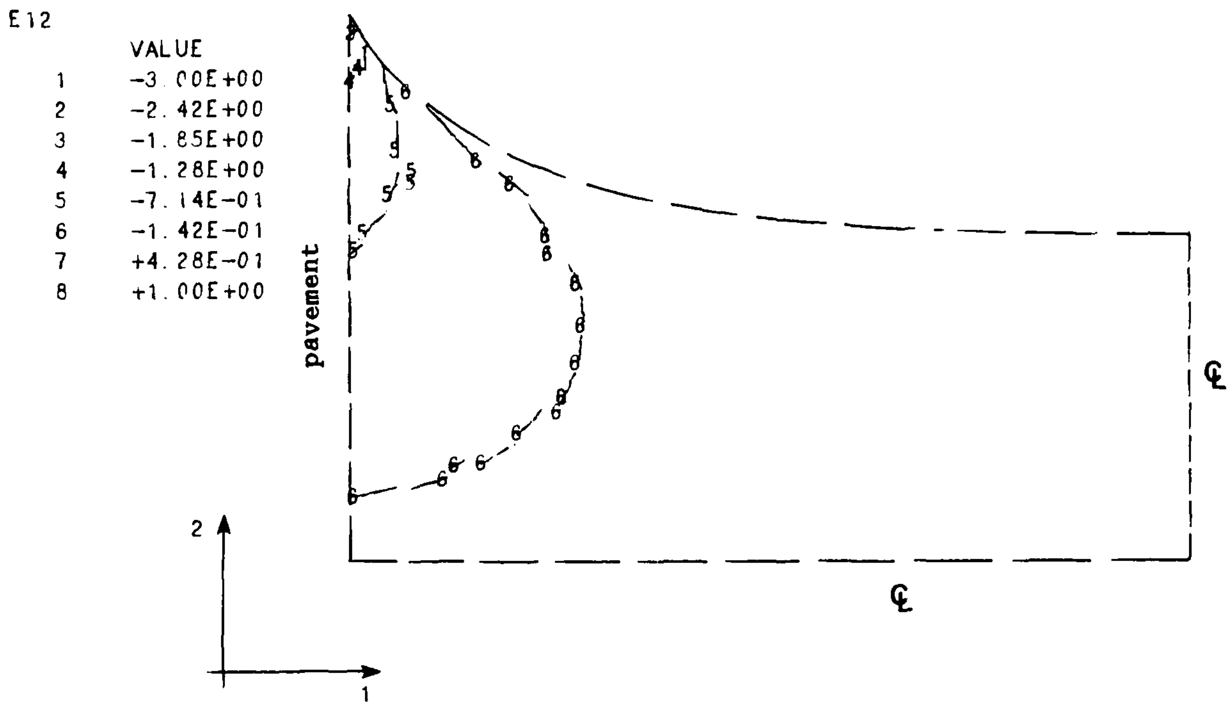

Figure 11. Shear strain (E12) for an extension of 50%.

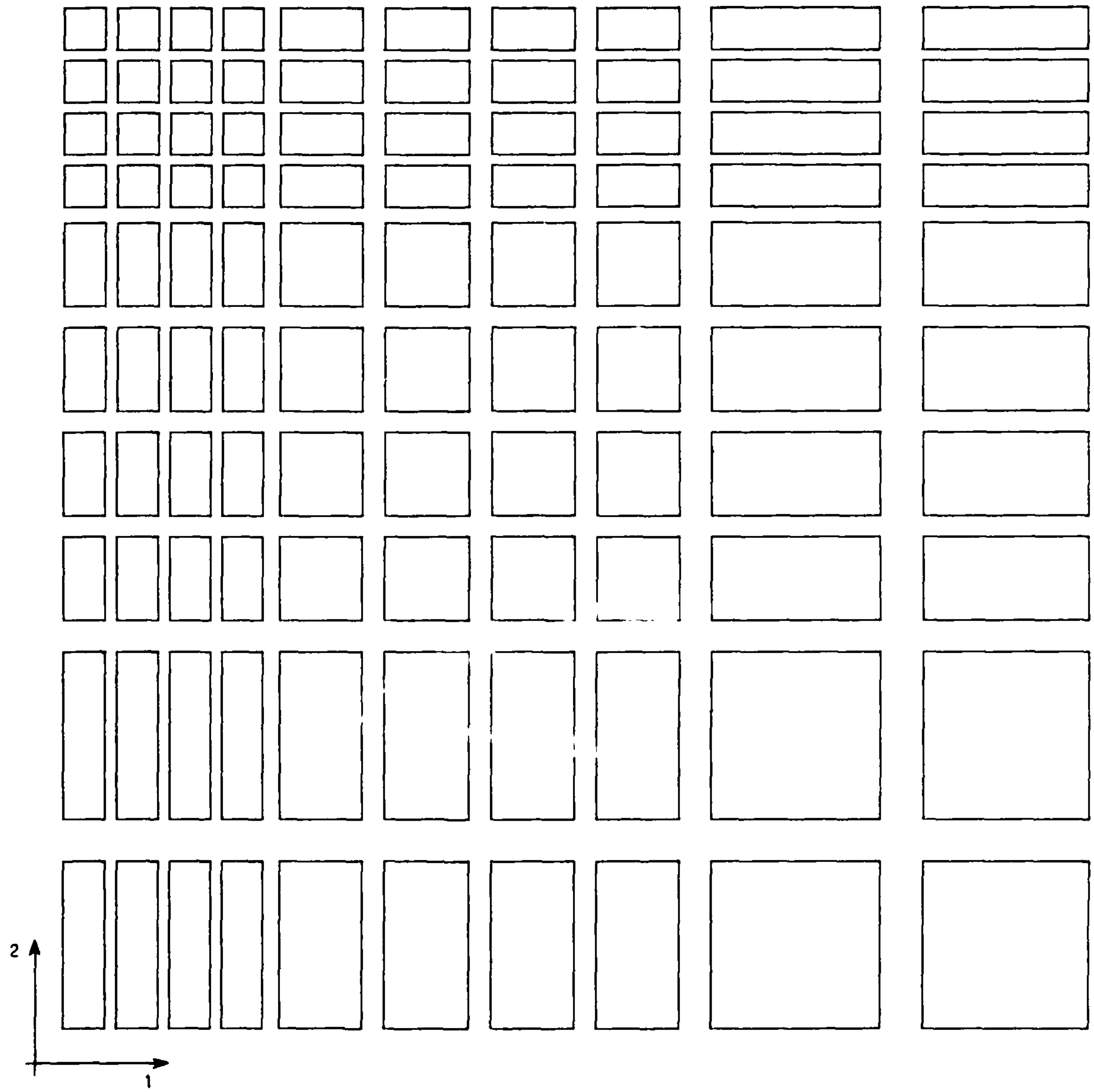

Figure 12. 10 by 10 finite element mesh no. 2 of a 1/4- by 1/4-inch pavement seal (symmetric quarter).

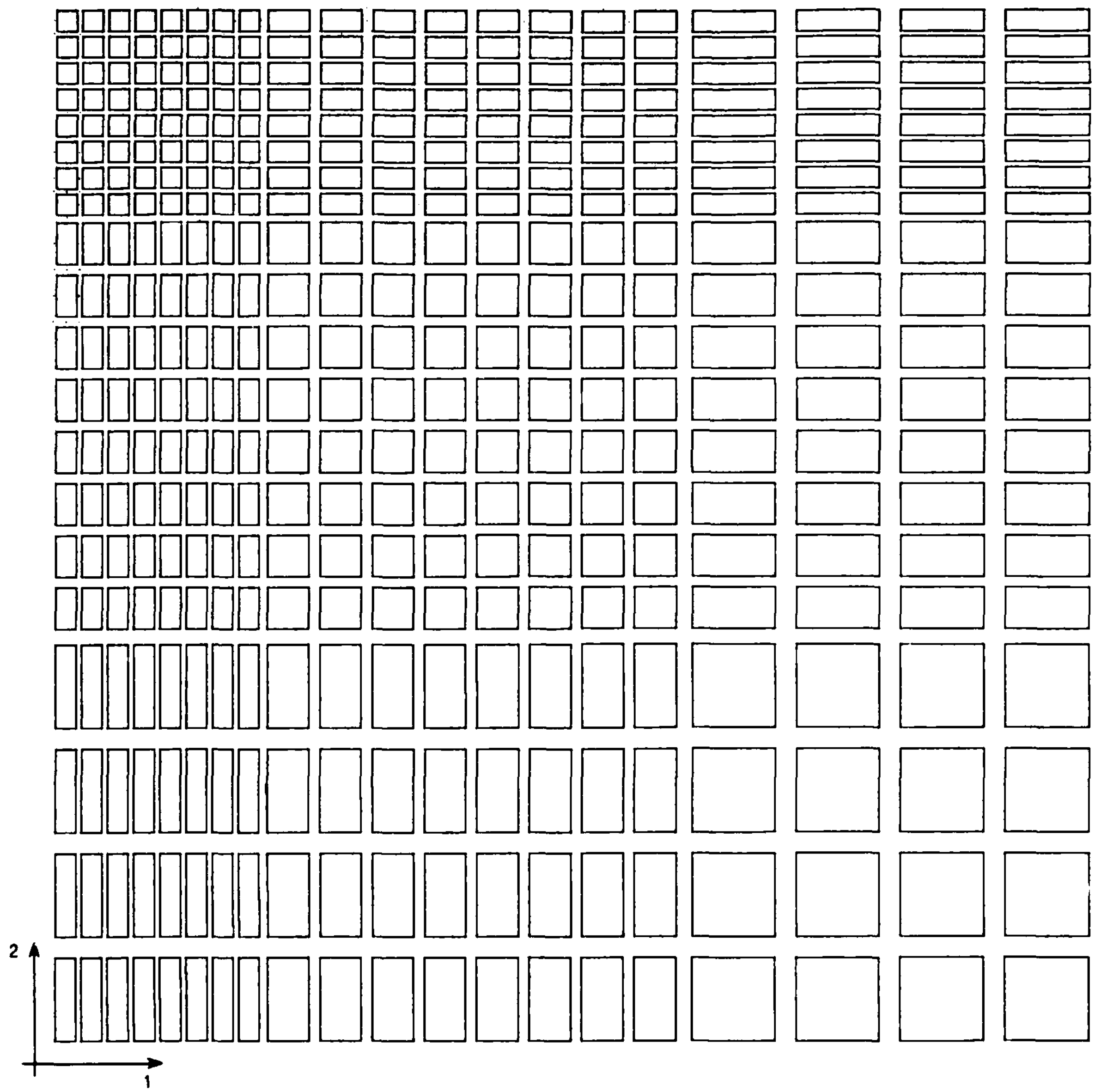

Figure 13. 20 by 20 finite element mesh no. 3 of a 1/4- by 1/4-inch pavement seal (symmetric quarter).

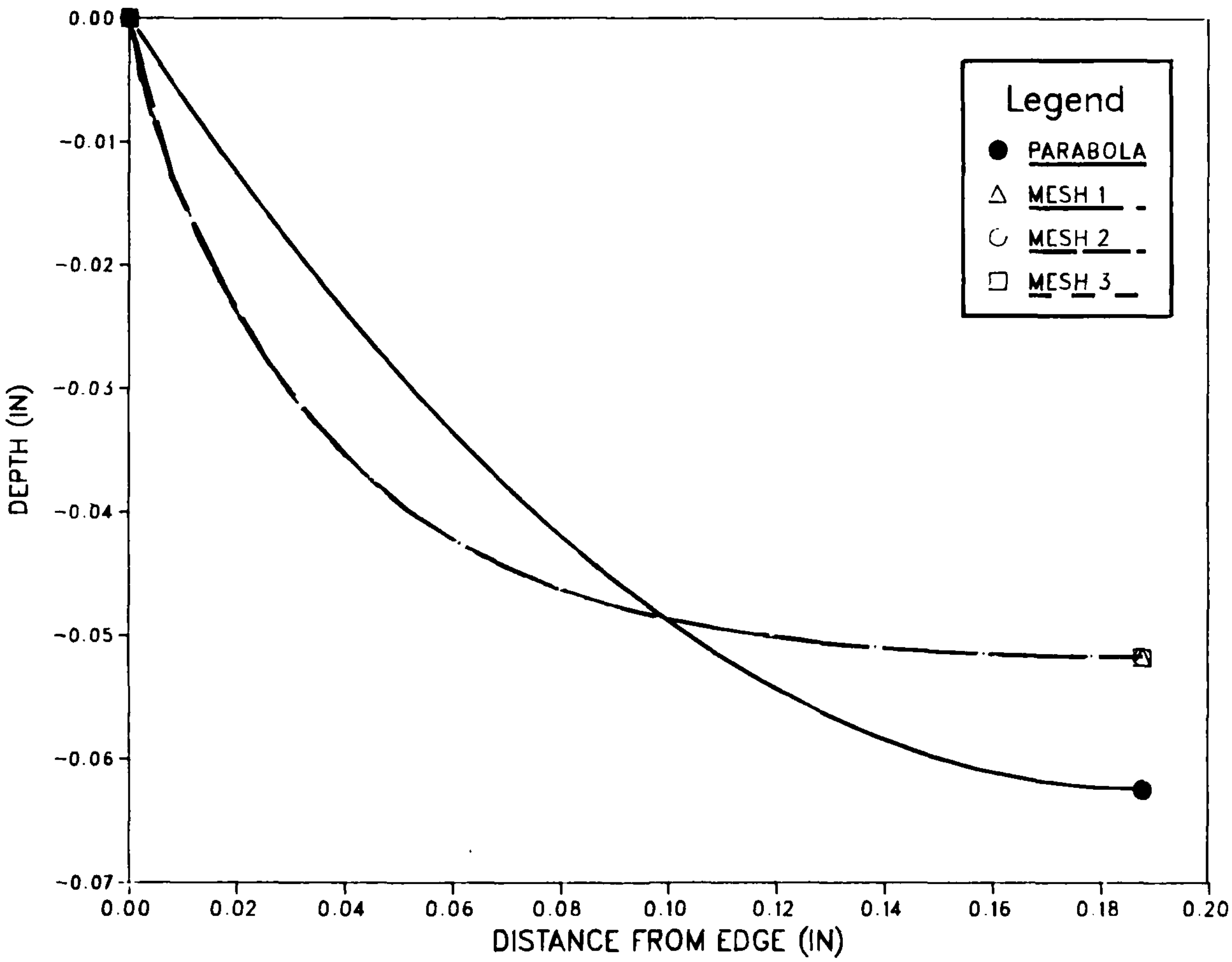

Figure 14. Free surface deformation for various finite element meshes of a 1/4- by 1/4-inch seal subjected to a 50% extension.

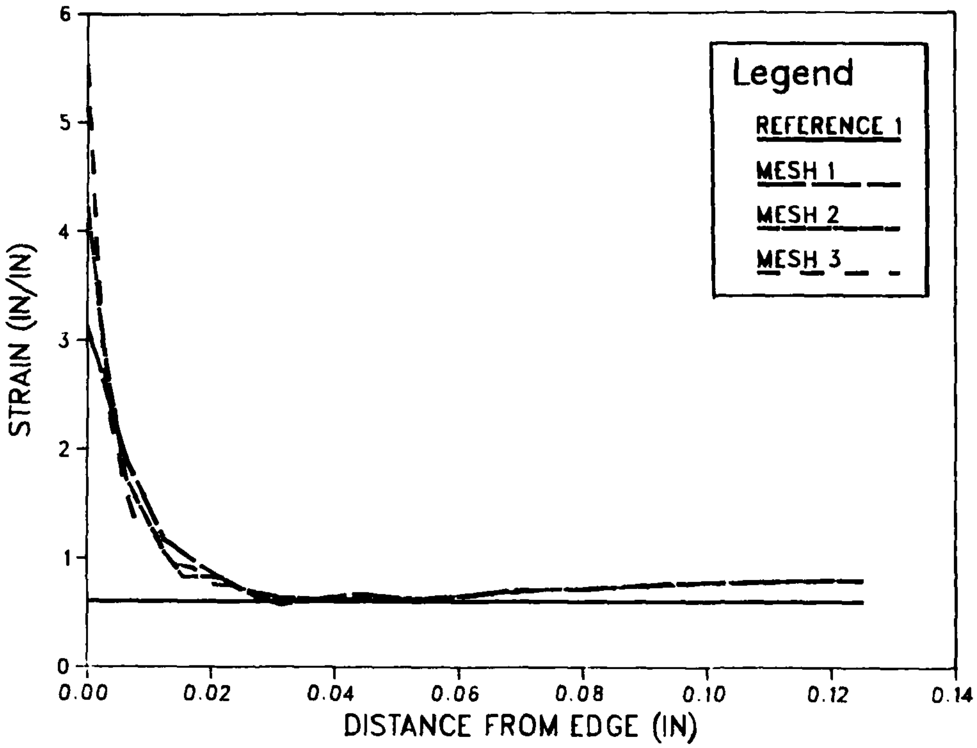

Figure 15. Strains on free surface for various finite element meshes of a 1/4- by 1/4-inch seal subjected to a 50% extension.

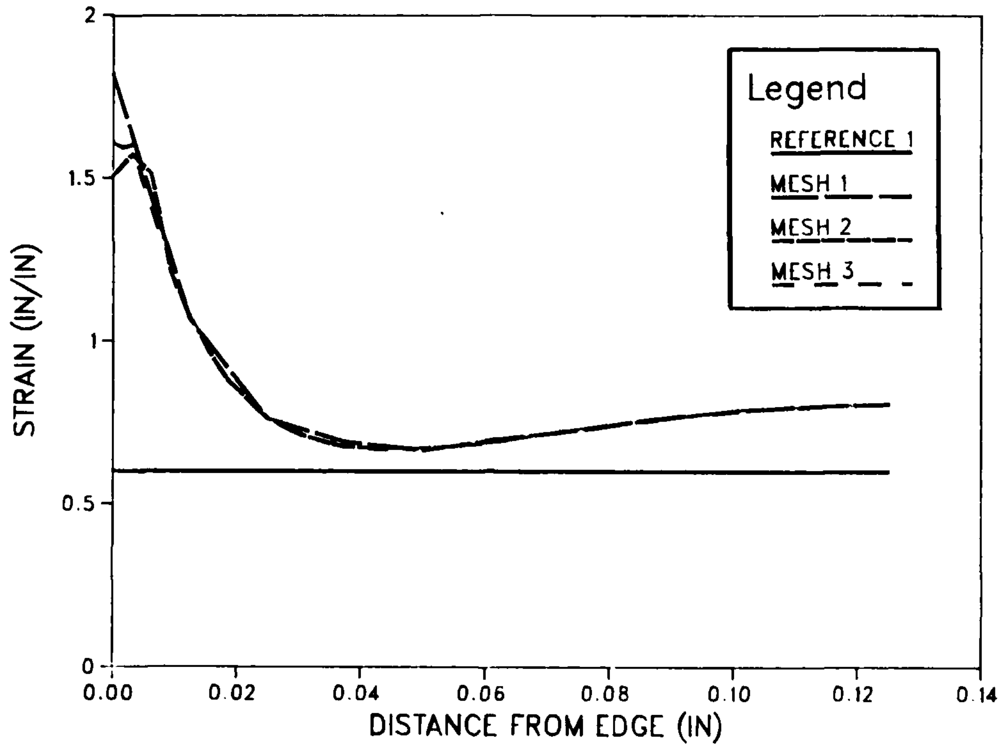

Figure 16. Strains at 0.00625 inches below the surface for various finite element meshes of a 1/4- by 1/4-inch seal subjected to a 50% extension.

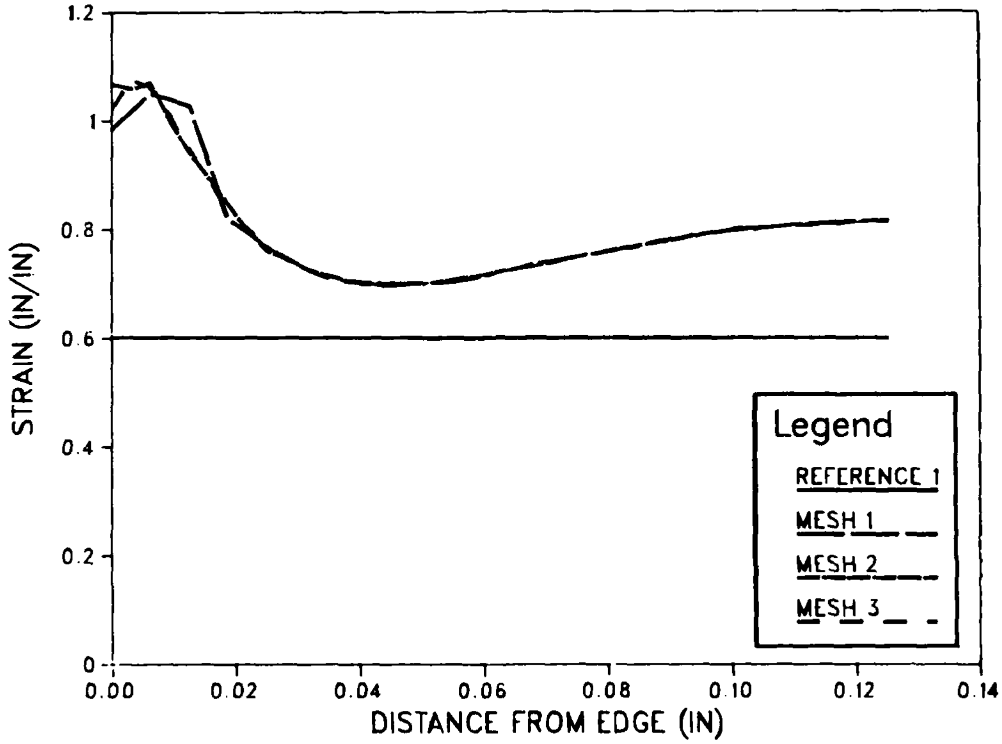

Figure 17. Strains at 0.0125 inches below the surface for various finite element meshes of a 1/4- by 1/4-inch seal subjected to a 50% extension.

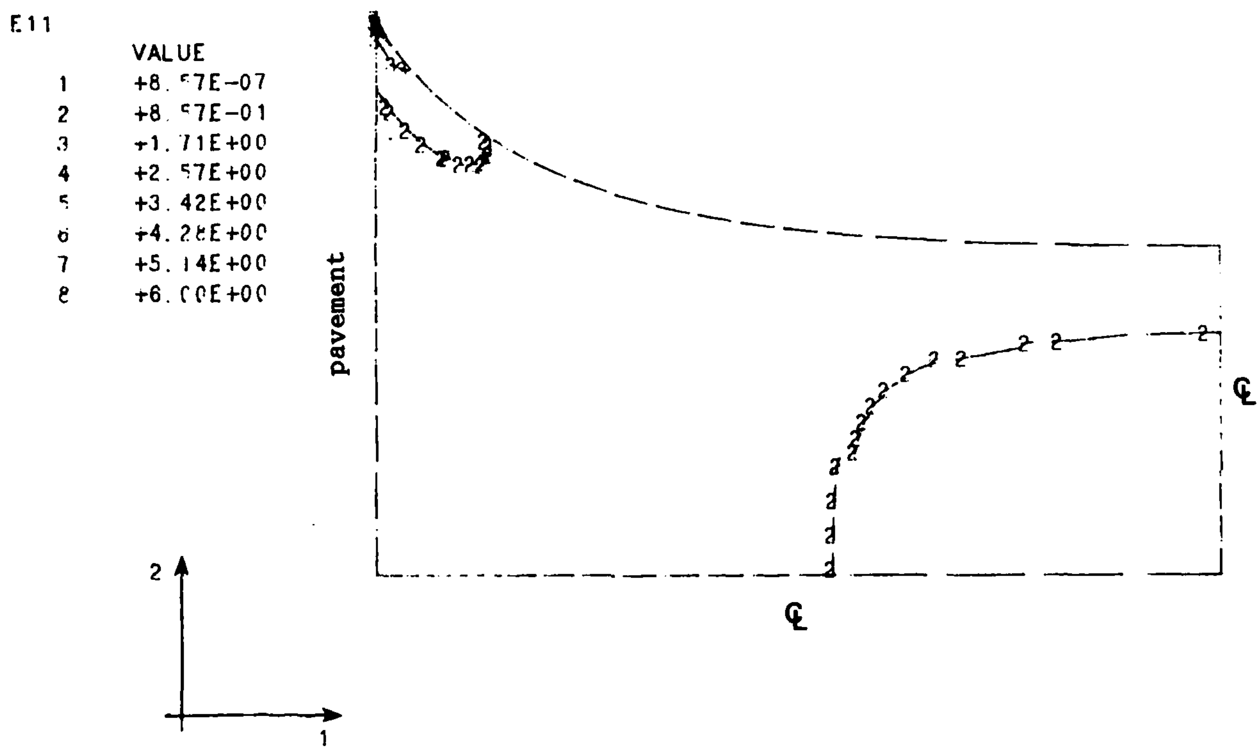

Figure 18. Typical plot of extension strains (E11) for a 1/4- by 1/4-inch pavement seal.

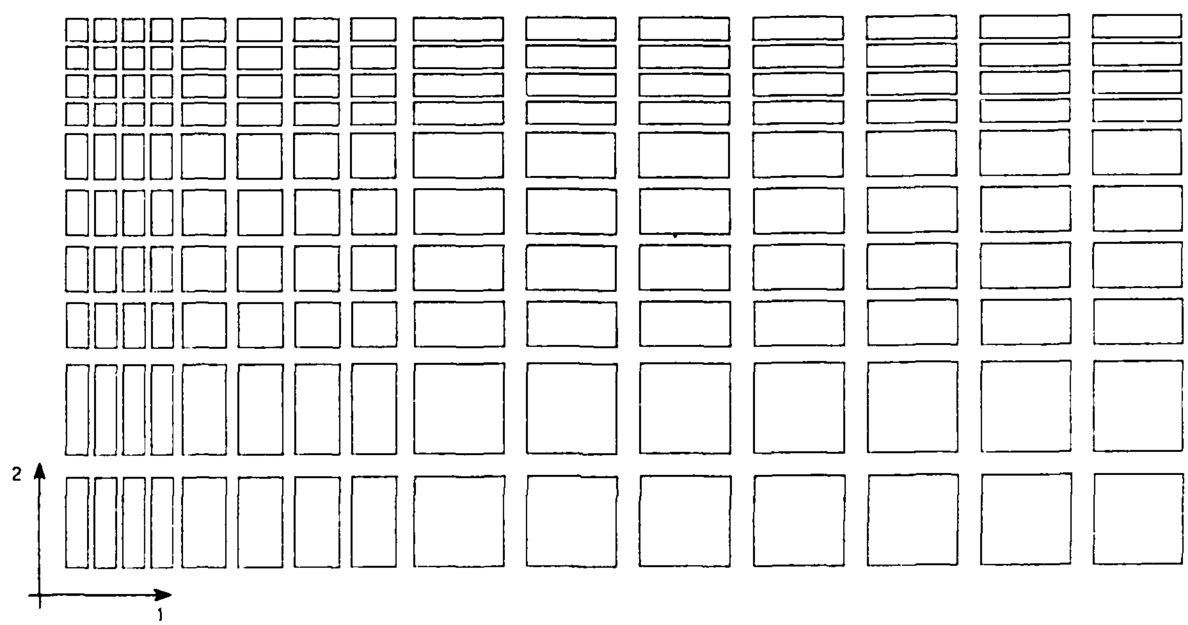

Figure 19. 10 by 15 finite element mesh of a 1/4-inch deep by 1/2-inch wide pavement seal (symmetric quarter).

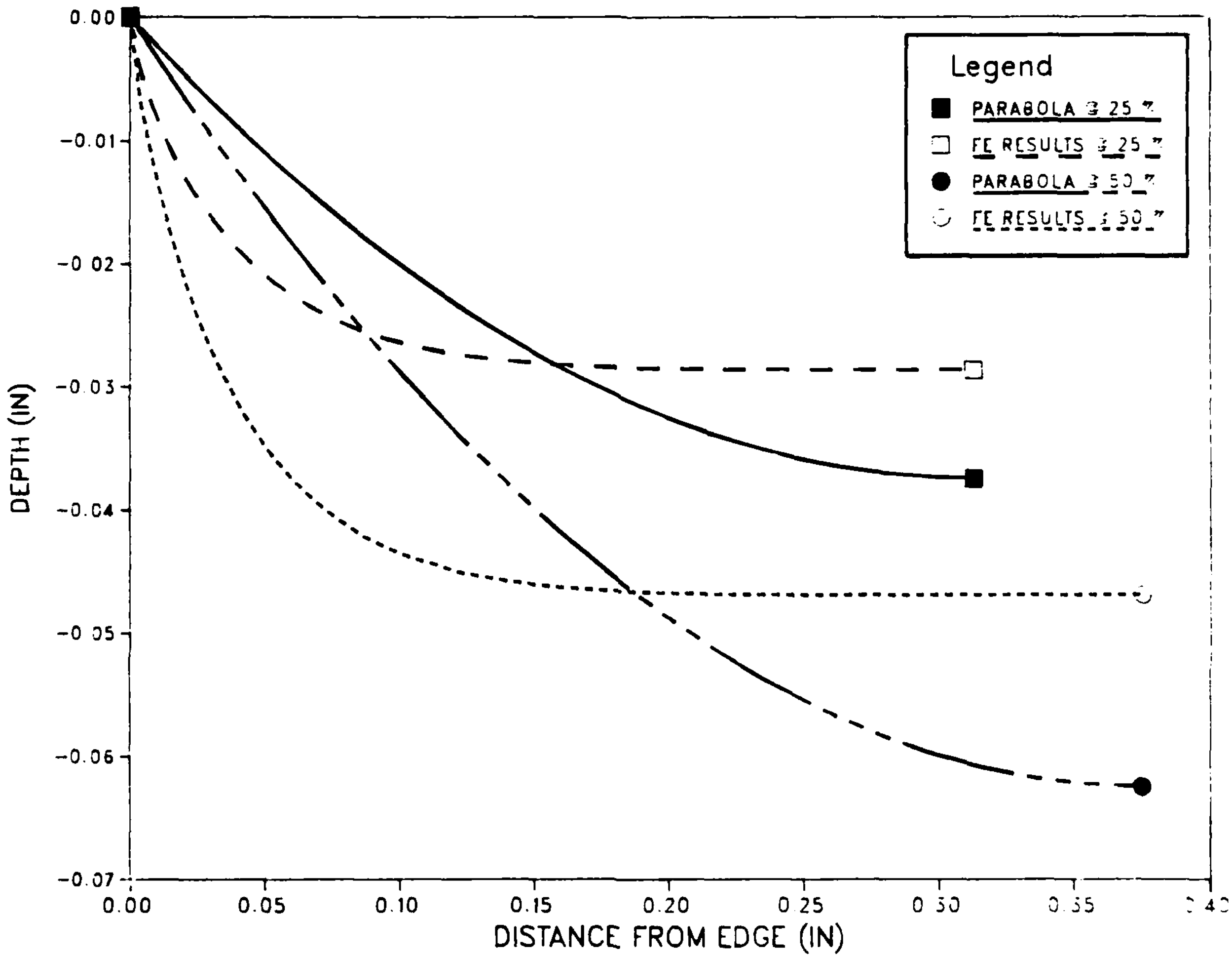

Figure 20. Free surface deformation of a 1/4-inch deep by 1/2-inch wide pavement seal subjected to 25% and 50% extensions.

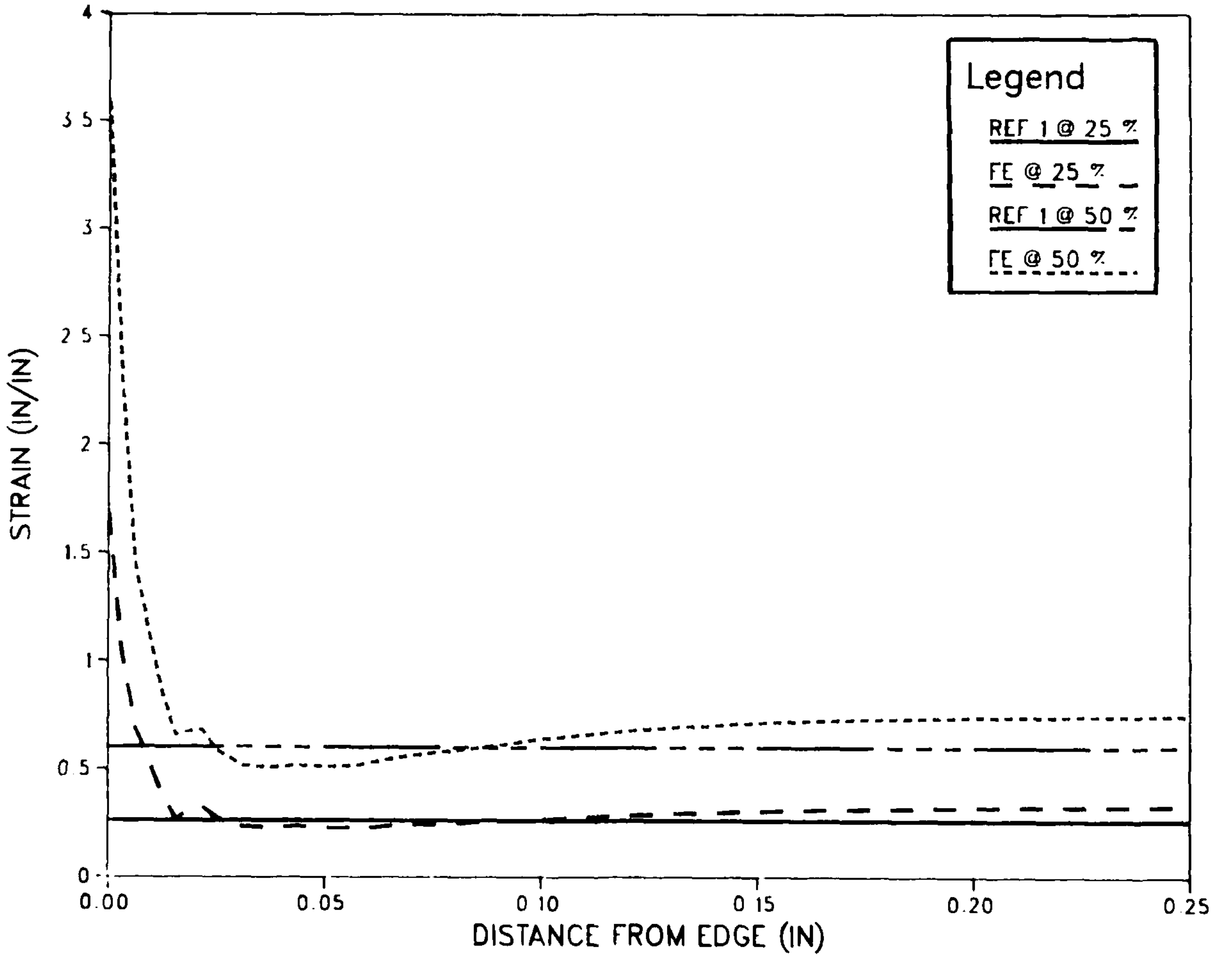

Figure 21. Strains on free surface of a 1/4-inch deep by 1/2-inch wide pavement seal subjected to 25% and 50% extensions.

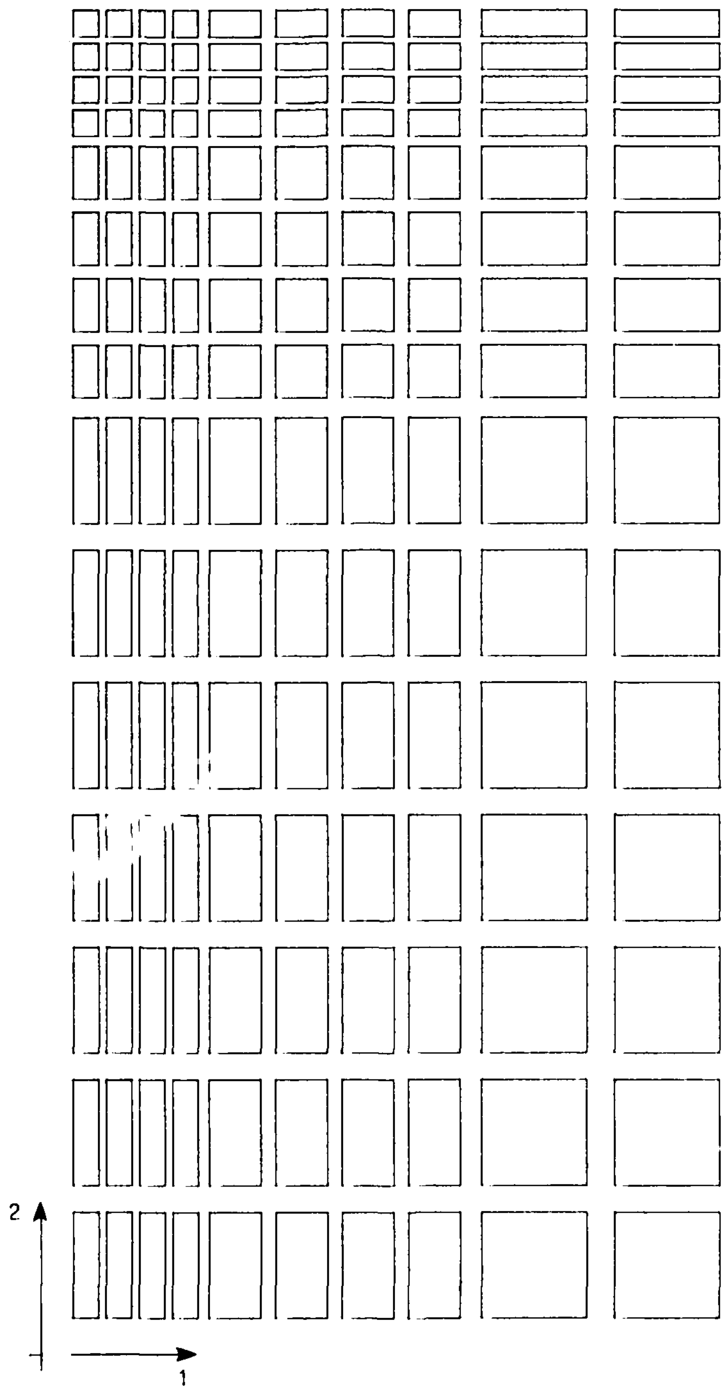

Figure 22. 15 by 10 finite element mesh of a 1/2-inch deep by 1/4-inch wide pavement seal (symmetric quarter).

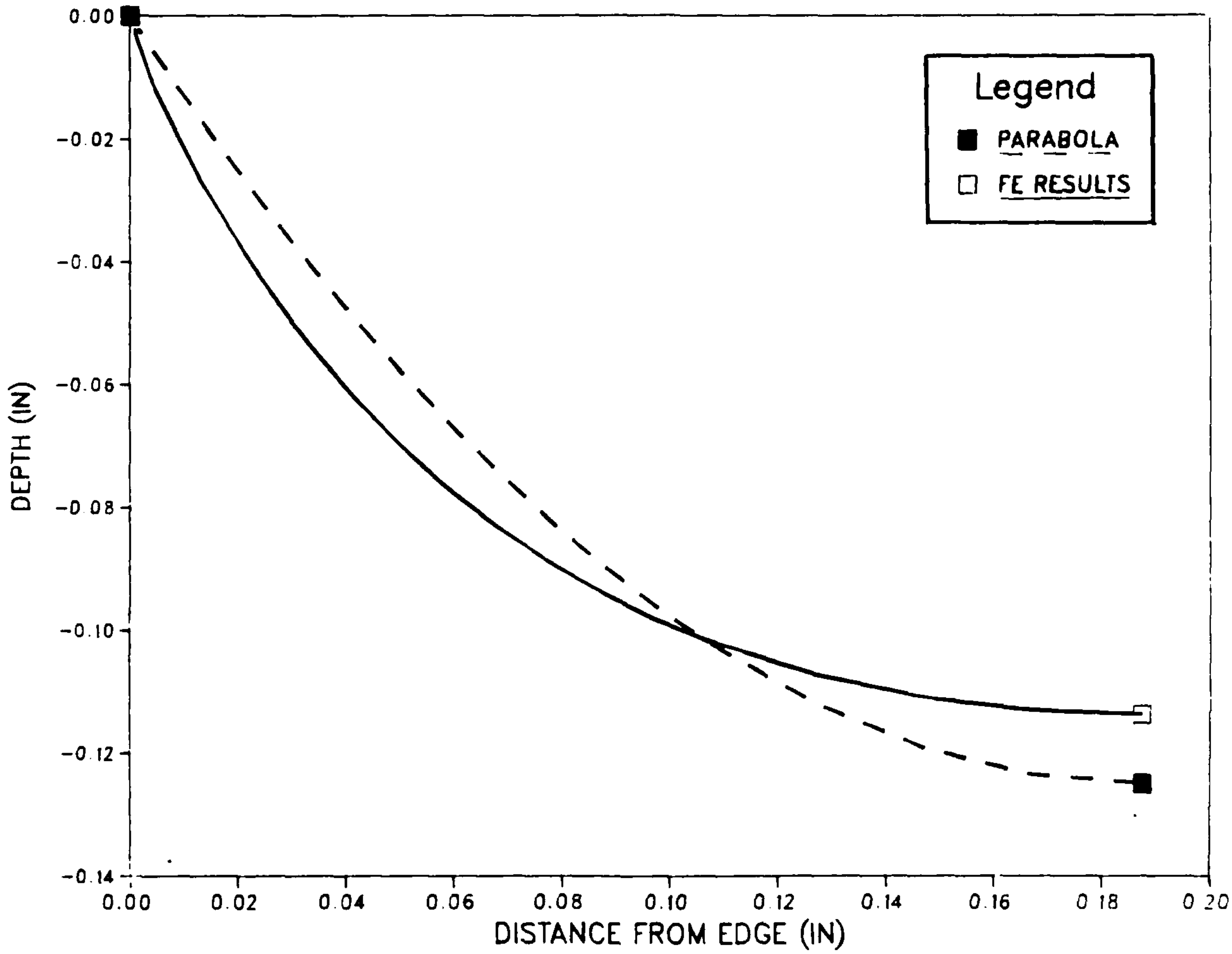

Figure 23. Free surface deformation of a 1/2-inch deep by 1/4-inch wide pavement seal subjected to 50% extension.

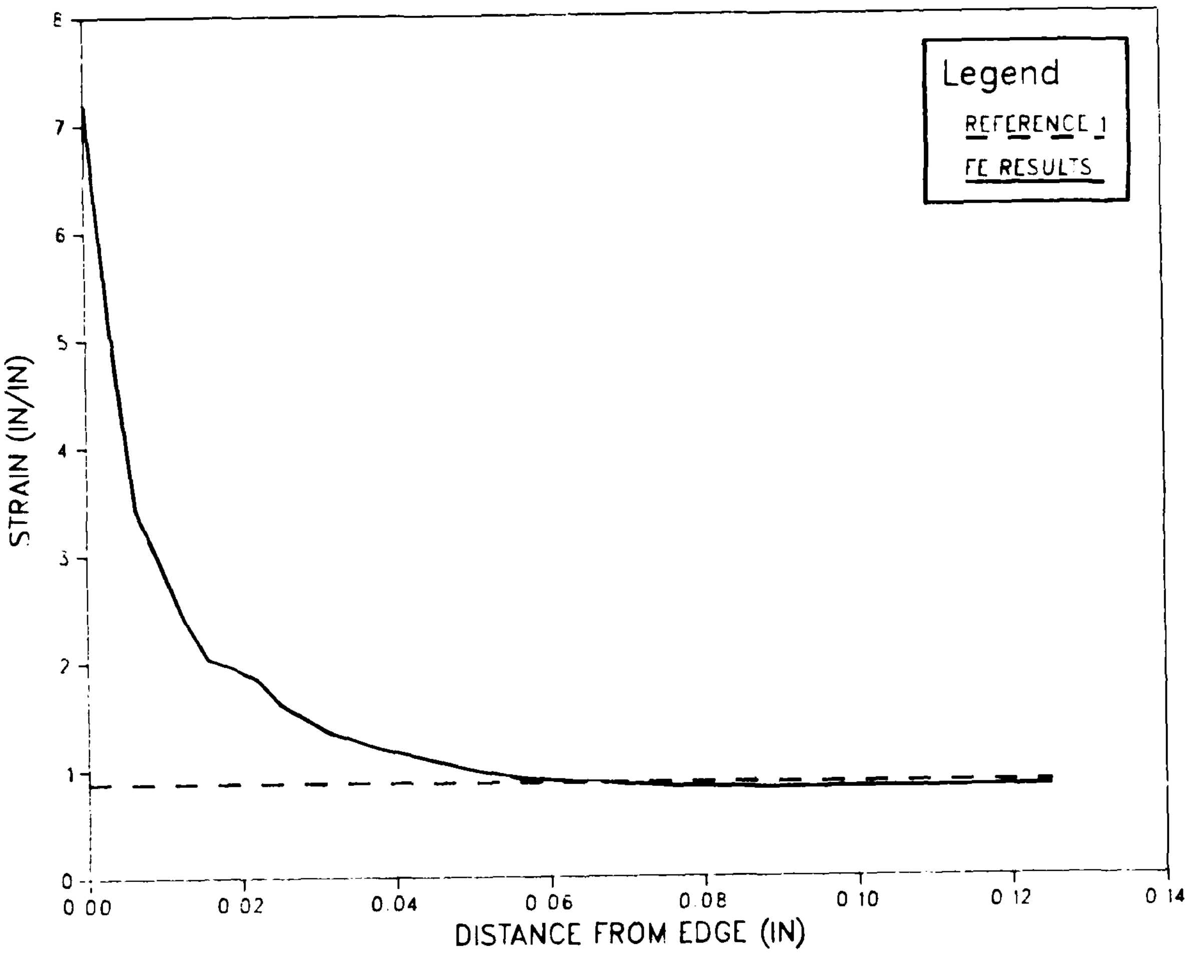

Figure 24. Strains on free surface of a 1/2-inch deep by 1/4-inch wide pavement seal subjected to 50% extension.

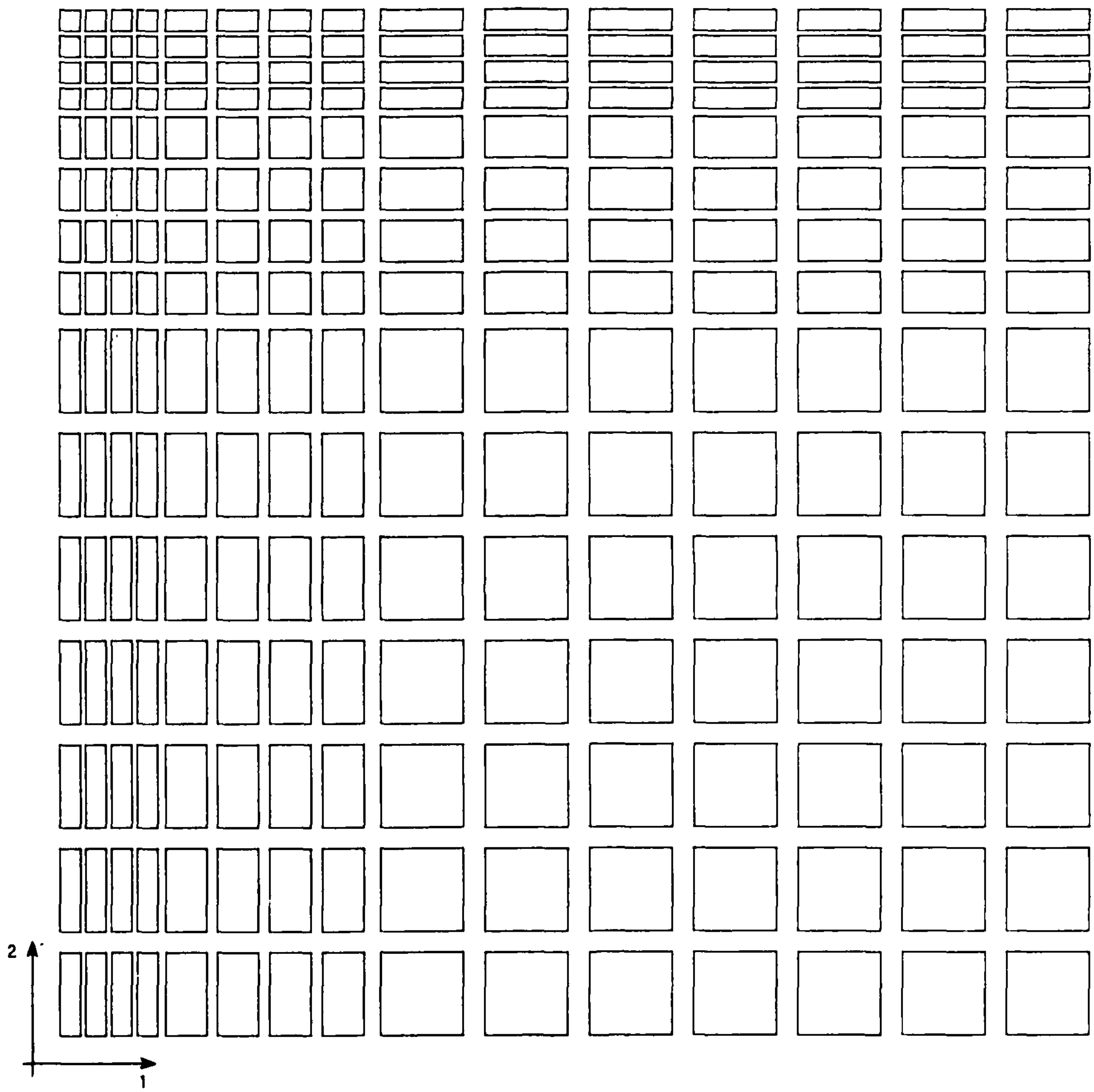

Figure 25. 15 by 15 finite element mesh of a 1/2- by 1/2-inch pavement seal (symmetric quarter).

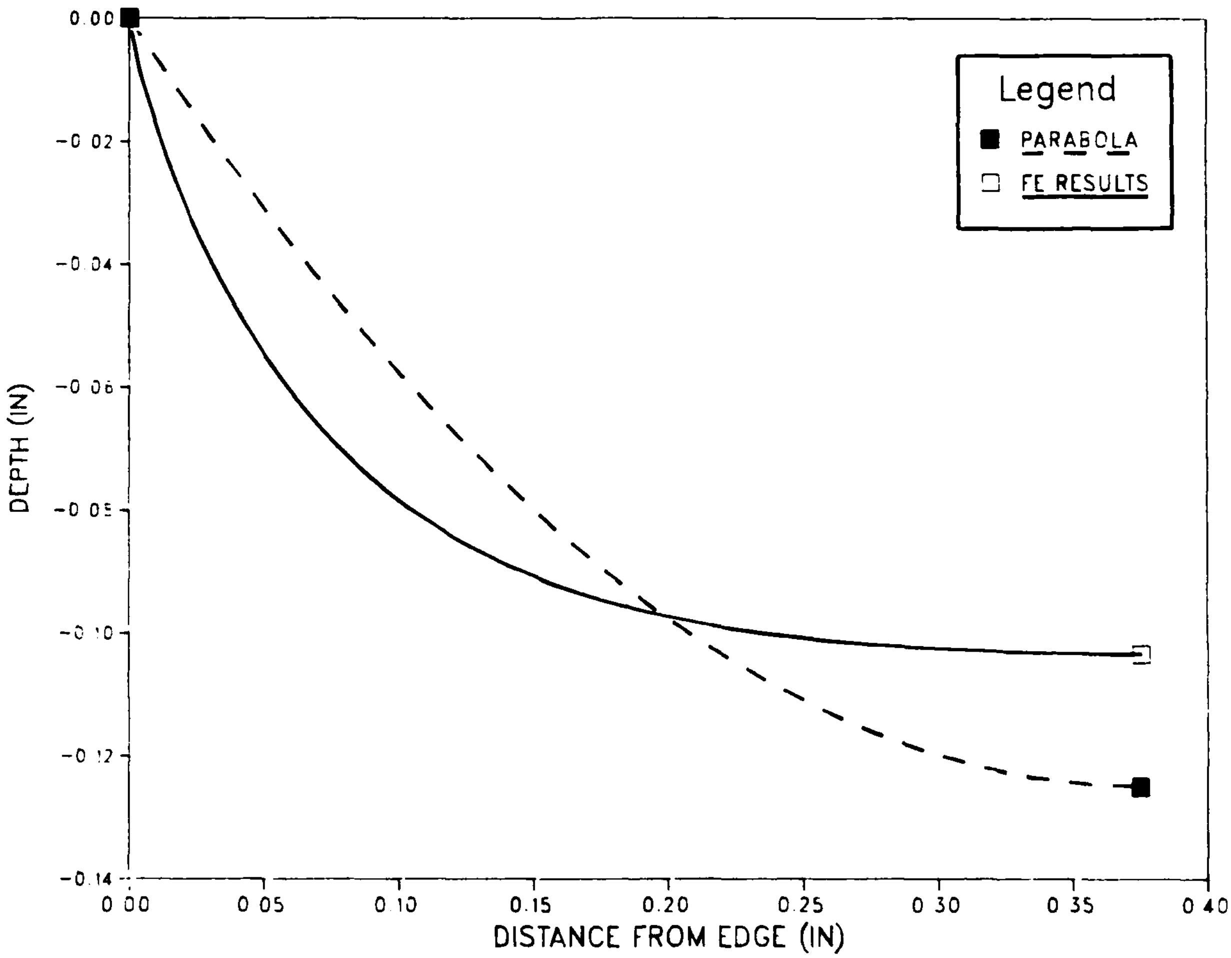

Figure 26. Free surface deformation of a 1/2- by 1/2-inch pavement seal subjected to 50% extension.

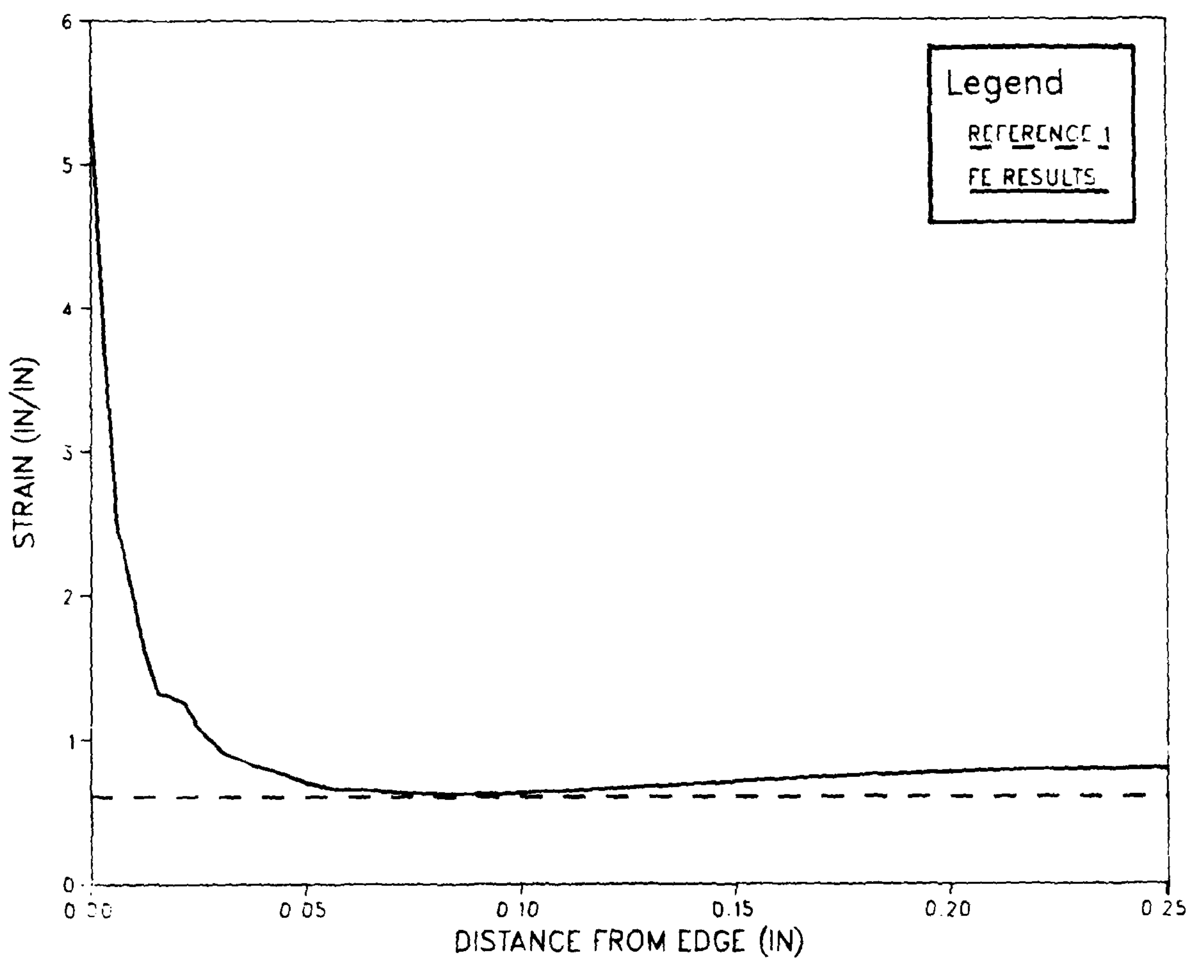

Figure 27. Strains on free surface of a 1/2- by 1/2-inch pavement seal subjected to 50% extension.

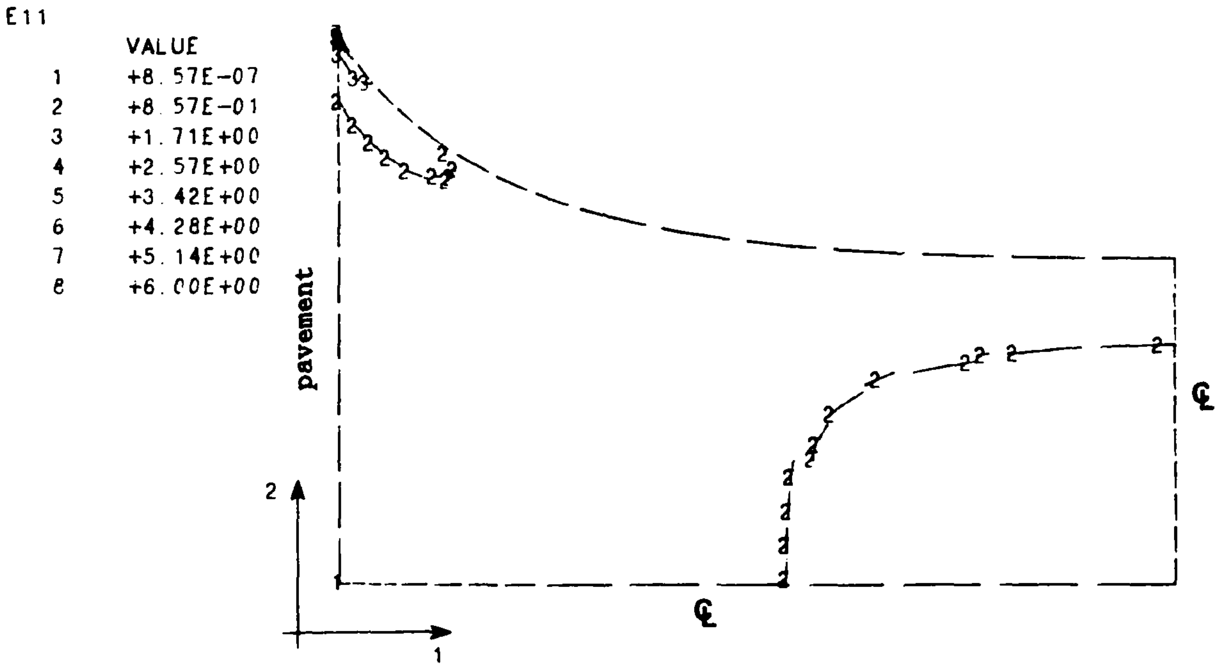

Figure 28. Contour plot of extension strains (E11) for a 1/2- by 1/2-inch pavement seal.

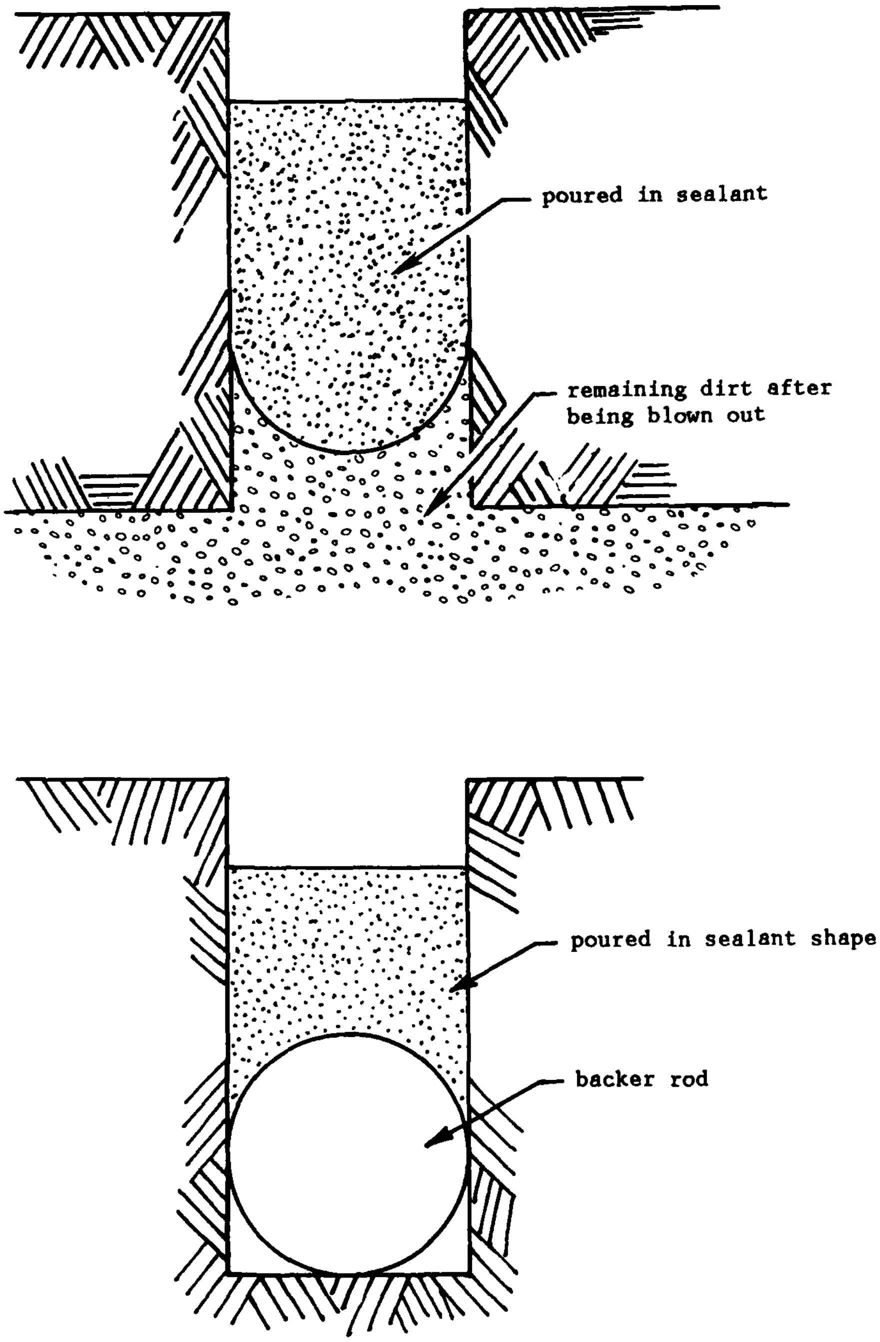

Figure 29. Possible variations in initial pavement seal shape.

DISTRIBUTION LIST

ARMY CERL Library, Champaign, IL
ARMY CRREL Library, Hanover, NH
ARMY EWES Library, Vicksburg MS; WESGP-E, Vicksburg, MS
DIRSSP Tech Lib, Washington, DC
DTIC Alexandria, VA
FAA Code APM-740 (Tomita), Washington, DC
LIBRARY OF CONGRESS Sci & Tech Div, Washington, DC
NAVCOASTSYSCEN Tech Library, Panama City, FL
NAVFACENGCOM Code 03, Alexandria, VA; Code 03T (Essoglou), Alexandria, VA; Code 04, Alexandria, VA; Code 04B1 (M.P. Jones), Alexandria, VA; Code 09M124 (Lib), Alexandria, VA; Code 1002B, Alexandria, VA
NAVFACENGCOM - CHES DIV, FPO-1PL, Washington, DC
NAVFACENGCOM - LANT DIV, Code 1112, Norfolk, VA; Code 405, Norfolk, VA; Library, Norfolk, VA
NAVFACENGCOM - PAC DIV, Code 405, Pearl Harbor, HI; Library, Pearl Harbor, HI
NAVFACENGCOM - SOUTH DIV, Code 4023, Charleston, SC; Library, Charleston, SC
NAVFACENGCOM - WEST DIV, Code 04A2.2 (Lib), San Bruno, CA; Code 102, San Bruno, CA; Code 405, San Bruno, CA; Code 411, San Bruno, CA
NAVSCOLCECOFF Code C35, Port Hueneme, CA
USDA For Svc, Tech Engrs, Washington, DC
CASE WESTERN RESERVE UNIV CE Dept (Perdikaris), Cleveland, OH
DAMES & MOORE Library, Los Angeles, CA
IOWA STATE UNIVERSITY CE Dept (Handy), Ames, IA
LOS ANGELES COUNTY PW Dept (J Vicelja), Alhambra, CA
MICHIGAN TECH UNIVERSITY CE Dept (Haas), Houghton, MI
MIT Lib, Tech Reports, Cambridge, MA
OREGON STATE UNIVERSITY CE Dept (Hicks), Corvallis, OR
PURDUE UNIVERSITY Engrg Lib, W. Lafayette, IN
SOUTHWEST RSCH INST M. Polcyn, San Antonio, TX
UNIVERSITY OF ILLINOIS Library, Urbana, IL
UNIVERSITY OF NEW MEXICO NMERI (Falk), Albuquerque, NM
VENTURA COUNTY PWA (Brownie), Ventura, CA
MC CLELLAND ENGRS, INC Library, Houston, TX
PORTLAND CEMENT ASSOC AE Fiorato, Skokie, IL
TRW INC Crawford, Redondo Beach, CA
WOODWARD-CLYDE CONSULTANTS West Reg, Lib, Oakland, CA

NCEL DOCUMENT EVALUATION

You are number one with us; how do we rate with you?

We at NCEL want to provide you our customer the best possible reports but we need your help. Therefore, I ask you to please take the time from your busy schedule to fill out this questionnaire. Your response will assist us in providing the best reports possible for our users. I wish to thank you in advance for your assistance. I assure you that the information you provide will help us to be more responsive to your future needs.

R. N. STORER, Ph.D, P.E.
Technical Director

DOCUMENT NO. __________ TITLE OF DOCUMENT: ______________________________

____

Date: __________ Respondent Organization : ______________________________

Name: ______________________ Activity Code: ______________________
Phone: ______________________ Grade/Rank: ______________________

Category (*please check*):

Sponsor _____ User _____ Proponent _____ Other (*Specify*) ______________________

Please answer on your behalf only; not on your organization's. Please check (*use an X*) only the block that most closely describes your attitude or feeling toward that statement:

SA Strongly Agree A Agree O Neutral D Disagree SD Strongly Disagree

---

	SA	A	N	D	SD
1. The technical quality of the report is comparable to most of my other sources of technical information.	( )	( )	( )	( )	( )
2. The report will make significant improvements in the cost and or performance of my operation.	( )	( )	( )	( )	( )
3. The report acknowledges related work accomplished by others.	( )	( )	( )	( )	( )
4. The report is well formatted.	( )	( )	( )	( )	( )
5. The report is clearly written.	( )	( )	( )	( )	( )
6. The conclusions and recommendations are clear and directly supported by the contents of the report.	( )	( )	( )	( )	( )
7. The graphics, tables, and photographs are well done.	( )	( )	( )	( )	( )

Do you wish to continue getting NCEL reports? ☐ YES ☐ NO

Please add any comments (e.g., in what ways can we improve the quality of our reports?) on the back of this form.

Comments:

Please fold on line and staple

DEPARTMENT OF THE NAVY

Naval Civil Engineering Laboratory
Port Hueneme, CA 93043-5003

Official Business
Penalty for Private Use $300

Code L03B
NAVAL CIVIL ENGINEERING LABORATORY
PORT HUENEME, CA 93043-5003

INSTRUCTIONS

The Naval Civil Engineering Laboratory has revised its primary distribution lists. The bottom of the label on the reverse side has several numbers listed. These numbers correspond to numbers assigned to the list of Subject Categories. Numbers on the label corresponding to those on the list indicate the subject category and type of documents you are presently receiving. If you are satisfied, throw this card away (or file it for later reference).

If you want to change what you are presently receiving:

- Delete - mark off number on bottom of label.
- Add - circle number on list.
- Remove my name from all your lists - check box on list.
- Change my address - line out incorrect line and write in correction **(DO NOT REMOVE LABEL)**.
- Number of copies should be entered after the title of the subject categories you select.

Fold on line below and drop in the mail.

Note: Numbers on label but not listed on questionnaire are for NCEL use only, please ignore them.

Fold on line and staple.

DEPARTMENT OF THE NAVY

Naval Civil Engineering Laboratory
Port Hueneme, CA 93043-5003

Official Business
Penalty for Private Use, $300

NO POSTAGE
NECESSARY
IF MAILED
IN THE
UNITED STATES

BUSINESS REPLY CARD

FIRST CLASS PERMIT NO. 12503 WASH D.C.

POSTAGE WILL BE PAID BY ADDRESSEE

Commanding Officer
Code L34
Naval Civil Engineering Laboratory
Port Hueneme, California 93043-5003

DISTRIBUTION QUESTIONNAIRE

The Naval Civil Engineering Laboratory is revising its Primary distribution lists.

SUBJECT CATEGORIES

1 SHORE FACILITIES
2 Construction methods and materials (including corrosion control, coatings)
3 Waterfront structures (maintenance/deterioration control)
4 Utilities (including power conditioning)
5 Explosives safety
6 Aviation Engineering Test Facilities
7 Fire prevention and control
8 Antenna technology
9 Structural analysis and design (including numerical and computer techniques)
10 Protective construction (including hardened shelters, shock and vibration studies)
11 Soil/rock mechanics
14 Airfields and pavements

15 ADVANCED BASE AND AMPHIBIOUS FACILITIES
16 Base facilities (including shelters, power generation, water supplies)
17 Expedient roads/airfields/bridges
18 Amphibious operations (including breakwaters, wave forces)
19 Over-the-Beach operations (including containerization, material transfer, lighterage and cranes)
20 POL storage, transfer and distribution

28 ENERGY/POWER GENERATION
29 Thermal conservation (thermal engineering of buildings, HVAC systems, energy loss measurement, power generation)
30 Controls and electrical conservation (electrical systems, energy monitoring and control systems)
31 Fuel flexibility (liquid fuels, coal utilization, energy from solid waste)
32 Alternate energy source (geothermal power, photovoltaic power systems, solar systems, wind systems, energy storage systems)
33 Site data and systems integration (energy resource data, energy consumption data, integrating energy systems)
34 ENVIRONMENTAL PROTECTION
35 Hazardous waste minimization
36 Restoration of installations (hazardous waste)
37 Waste water management and sanitary engineering
38 Oil pollution removal and recovery
39 Air pollution

44 OCEAN ENGINEERING
45 Seafloor soils and foundations
46 Seafloor construction systems and operations (including diver and manipulator tools)
47 Undersea structures and materials
48 Anchors and moorings
49 Undersea power systems, electromechanical cables, and connectors
50 Pressure vessel facilities
51 Physical environment (including site surveying)
52 Ocean-based concrete structures
54 Undersea cable dynamics

TYPES OF DOCUMENTS

85 Techdata Sheets 86 Technical Reports and Technical Notes
83 Table of Contents & Index to TDS
82 NCEL Guides & Abstracts
91 Physical Security

☐ None- remove my name